haematologica
Journal of The Ferrata Storti Foundation

Cellular and metabolic characteristics of pre-leukemic hematopoietic progenitors with GATA2 haploinsuficiency

by Avigail Rein, Ifat Geron, Eitan Kugler, Hila Fishman, Eyal Gottlieb, Ifat Abramovich, Amir Giladi, Ido Amit, Roger Mulet- Lazaro, Ruud Delwel, Stefan Gröschel, Smadar Levin-Zaidman, Nili Dezorella, Vered Holdengreber, Tata Nageswara Rao, Joanne Yacobovich, Orna Steinberg-Shemer, Qiu-Hua Huang, Yun Tan, Sai-Juan Chen, Shai Izraeli, and Yehudit Birger

Received: June 21, 2022.
Accepted: December 1, 2022.

Citation: Avigail Rein, Ifat Geron, Eitan Kugler, Hila Fishman, Eyal Gottlieb, Ifat Abramovich, Amir Giladi, Ido Amit, Roger Mulet- Lazaro, Ruud Delwel, Stefan Gröschel, Smadar Levin-Zaidman, Nili Dezorella, Vered Holdengreber, Tata Nageswara Rao, Joanne Yacobovich, Orna Steinberg-Shemer, Qiu-Hua Huang, Yun Tan, Sai-Juan Chen, Shai Izraeli, and Yehudit Birger. Cellular and metabolic characteristics of pre-leukemic hematopoietic progenitors with GATA2 haploinsuficiency. Haematologica. 2022 Dec 8. doi: 10.3324/haematol.2022.279437 [Epub ahead of print]

Cellular and metabolic characteristics of pre-leukemic hematopoietic progenitors with GATA2 haploinsuficiency

Avigail Rein[1,2,3], Ifat Geron[1,2,3,4], Eitan Kugler[1,2,3], Hila Fishman[1,2,3], Eyal Gottlieb[5], Ifat Abramovich[5], Amir Giladi[6], Ido Amit[6], Roger Mulet- Lazaro[7], Ruud Delwel[7,8], Stefan Gröschel[7,9,10], Smadar Levin-Zaidman[11], Nili Dezorella[11], Vered Holdengreber[12], Tata Nageswara Rao[13], Joanne Yacobovich[2], Orna Steinberg-Shemer[2,4], Qiu-Hua Huang[14], Yun Tan[14], Sai-Juan Chen[14], Shai Izraeli[1,2,3,4] and Yehudit Birger[1,2,3,4]

Affiliations

[1]Department of Human Molecular Genetics and Biochemistry, Sackler Medical School, Tel Aviv University, Tel Aviv 69978, Israel;

[2]The Rina Zaizov Division of Pediatric Hematology-Oncology, Schneider Children's Medical Center, Petah Tikva; Israel

[3]Functional Genomics and Childhood Leukaemia Research, Sheba Medical Centre, Tel-Hashomer, Israel

[4]Felsenstein Medical Research Center, Sackler School of Medicine Tel-Aviv University, Petah Tikva; Israel

[5]Technion Integrated Cancer Center, Faculty of Medicine, Technion Israel Institute of Technology, Haifa, Israel

[6]Department of Immunology, Weizmann Institute of Science, Rehovot, Israel;

[7]Department of Hematology, Erasmus University Medical Center, Rotterdam, 3015 GE, the Netherlands

[8]Oncode Institute, Erasmus University Medical Center, Rotterdam, the Netherlands;

[9]Molecular Leukemogenesis, Deutsches Krebsforschungszentrum, 69120 Heidelberg, Germany

[10]Department of Internal Medicine V, Heidelberg University Hospital, Heidelberg, Germany

[11]Electron Microscopy Unit, Weizmann Institute of Science, Rehovot, Israel

[12]Electron Microscopy Unit, IDRFU, Faculty of Life Sciences, Tel Aviv University, Israel

[13]Stem Cells and Leukemia Laboratory, University Clinic of Hematology & Central Hematology, Department of Biomedical Research (DBMR), Inselspital Bern, University of Bern, Switzerland

[14]State Key Laboratory of Medical Genomics, Shanghai Institute of Hematology, Rui Jin Hospital, Jiao Tong University School of Medicine, Shanghai 200025, China.

Running title: Gata2 preleukemia

Corresponding authors:

Shai Izraeli, The Rina Zaizov Pediatric Hematology Oncology Division, Schneider Children's Medical Center of Israel 14 Kaplan St, Petach Tiqva, 49202 Israel. Phone number: 972-52-6666360, sizraeli@gmail.com. Orchid identifier 000000026938-2540

Yehudit Birger, The Rina Zaizov Pediatric Hematology Oncology Division, Schneider Children's Medical Center of Israel 14 Kaplan St, Petach Tiqva, 49202 Israel, yehudit.birger@gmail.com

Data Sharing Statement

Raw data is available in GEO through accession GSE143238 at: https://www.ncbi.nlm.nih.gov/geo/query/acc.cgi?acc=GSE143238. And on GEO through accession GSE143308 https://www.ncbi.nlm.nih.gov/geo/query/acc.cgi?acc=GSE143308

Word count: Abstract: 235 words; Main text: 3773 words; 6 figures; 1 supplementary file.

Authorship Contributions

S.I. D.B and A.R. designed research; A.R., Y.B, I.G., E.K, H.F. I.A[4], performed research; S.J.C., R.D.,S.G, R.M.L, S.L.Z, N.D, V.H, I.A[5], J.Y, O.S.S, Q.H., Y.T and E.G., contributed new reagents/analytic tools; A.R., A.G, I.G., Y.B., E.G, R.D. I.A[5], R.M.L, T.N.R, S.J.C, Q.H., Y.T and S.I. analyzed data; and A.R. D.B and S.I, wrote the paper.

Disclosure of Competing Interests

The Authors declare no competing Interests.

Acknowledgments

This study was supported by the Israel Science Foundation and the National Science Foundation China to SI and SJC, Israeli Ministry of Science and DKFZ (SI, SG), the Waxman Cancer Research Foundation (SI), the Ministry of Health (SI), Larger Than Life Foundation (SI, AR), Hans Neufeld Stiftung (SI) and ICCF (SI). We thank professor Atan Gross for his invaluable advice regarding mitochondrial metabolism and analysis, Jonatan Barel from the for RNAseq analysis and to Hadas

Keren-Shaul for 10X RNA sequencing services. We are indebted to Itzhak Ben Moshe and Erez Shtosel, for mouse care and past and present members of S.I. research group for fruitful discussions and advice.

This work was performed in partial fulfilment of the requirements for a PhD degree of Avigail Rein, Sackler Faculty of Medicine, Tel Aviv University, Israel

Abstract

Mono-Allelic germline disruptions of the transcription factor GATA2 result in a propensity for developing myelodysplastic syndrome (MDS) and acute myeloid leukemia (AML) affecting more than 85% of carriers. How a partial loss of GATA2 functionality enables leukemic transformation occurring years later in life, is unclear. This question is unsolved mainly due to lack of informative models, as Gata2 heterozygote mice do not develop hematologic malignancies. Here we show that two different germline Gata2 mutations (tgERG/GATA2^{het} and tgERG/Gata2^{L359V}) accelerate AML in mice expressing the human hematopoietic stem cell regulator ERG. Analysis of ERG/Gata2$^{\mathbf{het}}$ fetal liver and bone marrow derived hematopoietic cells revealed a distinct pre-leukemic phenotype. This was characterized by enhanced transition from stem to progenitor state, increased proliferation, and a striking mitochondrial phenotype, consisting of highly expressed Oxidative-Phosphorylation related gene-sets, elevated oxygen consumption rates, and notably, markedly distorted mitochondrial morphology. Importantly, the same mitochondrial gene-expression signature was observed in human AMLs harboring GATA2 aberrations. Similar to the observations in mice, non-leukemic bone marrows from children with germline GATA2 mutation demonstrated marked mitochondrial abnormalities. Thus, we observed the tumor suppressive effects of GATA2 in two germline Gata2 genetic mouse models. As oncogenic mutations often accumulate with age, Gata2 deficiency mediated priming of hematopoietic cells for oncogenic transformation may explain the earlier occurrence of MDS/AML in patients with GATA2 germline mutation. The mitochondrial phenotype is a potential therapeutic opportunity for prevention of leukemic transformation in these patients.

Introduction

The hematopoietic transcriptional machinery is a network of highly tuned feedback circuits. Dysfunction of a pivotal regulator might therefore hinder its entire performance. GATA2 is a cardinal hematopoietic transcription factor critical for initiation of fetal hematopoiesis and for maintaining hematopoietic stem cells pool throughout life by restricting stem cells differentiation [1-3].

Abnormal regulation of GATA2 expression and somatic mutations in GATA2 have been associated with both tumor promotion and tumor inhibition [4, 5] .Yet germline heterozygous mutations in GATA2, most of which are loss-of-function, are uniformly associated with increased risk for myeloid malignancies [6, 7]. GATA2 germline haploinsufficiency syndrome is a multisystem disorder highly variable in clinical presentation [8, 9]. Albeit versatile, the most common and gravest consequence of the disorder is the propensity to develop MDS /AML, which affects more than 80% of diagnosed carriers before the age of forty [8, 10, 11]. More than 150 unique mutations have been associated with GATA2 haploinsufficiency [8, 11, 12] including missense-substitutions, nonsense-truncations, and small indels. Additional secondary oncogenic changes often contribute for leukemic transformation. Hence, the optimal timing of bone marrow transplantation, currently the sole therapeutic strategy for *GATA2* deficiency, is unclear.

Thus, there is an unmet need to decipher cellular events that precedes malignancy in carriers of germline GATA2 mutations. One of the problems is paucity of pre-clinical models. While total ablation of murine Gata2 confers embryonic lethality [2, 13], heterozygous mice display only a mild phenotype and develop neither MDS nor leukemia [13, 14]. As hematopoietic malignancies in patients with germline GATA2 abnormalities are characterized by additional somatic oncogenic mutations, it is reasonably to hypothesize that the tumor suppressive effect of Gata2 deficiency will

be revealed in mice expressing a hematopoietic oncogene. Interestingly, germline Gata2 haploinsufficiency delayed the occurrence of leukemia in mice carrying CbfbMYH11 fusion [15] while accelerating leukemogenesis in mice expressing Evi1 [16] or loss of C/Ebp alpha [17], respectively. These later studies focused on detailed analysis of the mouse leukemias but not on the pre-leukemic phenotype.

Here we report a detailed analysis of the impact of Gata2 deficiency on hematopoietic stem and progenitor cells (HSPCs) at the pre-leukemic phase. We examined the hypothesis that the implication of dysfunctional Gata2 in mice would be maximized upon expression of a stem cell oncogene. ERG, an hematopoietic Ets transcription factor that is up-stream regulator of GATA2 [18] is a potent regulator of normal and leukemic stem cells [19, 20]. ERG has been recently shown to be the main driver of AML caused by haploinsufficiency of GATA2 with increased expression of EVI-1[21]. Accordingly, we have traced the trajectories of HSPCs with heterozygous germline *Gata2* deficiency from gestation to leukemia in ERG transgenic mice. We show that the loss of Gata2 caused early expansion of proliferative hematopoietic progenitor cells detected already at the fetal liver stage long before overt leukemic transformation. We further discovered that the haploinsufficiency of Gata2 induced a mitochondrial phenotype in these preleukemic cells. Significantly, this was confirmed in children with germline GATA2 haploinsufficiency, and in human AMLs with GATA2 mutations.

Methods

Mice handling

Double transgenic mice were generated by crossing tgERG [18] (from two different tgERG F_1) mice with *Gata2*^{het} mice (provided by Stuart Orkin [2]) or with *Gata2*$^{+/L359V}$

knock-in mice, provided by Sai-Juan Chen[22]. See detailed description of the mouse model in supplementary methods. Studies were approved by the institutional animal care and use committee (1149/18/ANIM).

Immunophenotyping

BM cells were washed in 2% FBS in PBS and re-suspended in 100 µl staining media (STM) containing fluorochrome conjugated antibodies for 30 min. Following staining, cells were washed, re-suspended to a final volume of 100µl STM and analyzed by Gallios 3 laser/10 colors Flow Cytometer (Beckman coulter, Brea, California, USA). Leukemia panels are detailed in the supplemental methods.

Histopathology

Femurs and Spleens were fixed in 4% neutral buffered formalin, paraffin-embedded, and stained with hematoxylin and eosin using standard protocols.

Methylcellulose re-plating assays

E14.5 fetal liver (FL) cells were harvested and forced through 70µm filter strainer into 2% Fetal Calf Serum in PBS at 4^{o}C. Lineage negative cells enrichment was performed using MACS magnetic columns (MACS Miltenyi Biotec, Bergisch Gladbach, Germany). 2X10^{4} cells were plated in methylcellulose supplemented with IL6, IL3 and SCF (Stem Cell Technologies, Vancouver, Canada, MethoCult GF M3534) in duplicates. After seven days, colonies (>50 cells) were counted and re-suspended, cells counted and re-plated in same manner until colonies were no longer formed. Three independent experiments were performed, each with 2-3 FLs from each genotype.

10X RNA sequencing

BM derived single-cell suspension was prepared from each mouse femur, diluted to a concentration of ~1000 cells/µl and loaded into the 10x Chromium microfluidics

system, aiming for 5000 single cells/sample. An RNA-seq library was prepared for each sample according to the manufacturer's protocol. Final libraries were sequenced using the Nextseq 75 cycles high output kit (Illumina) for a coverage of 50000 reads/cell. Single cell RNA-seq data analysis is detailed in the supplemental methods. Raw data is available on GEO through accession GSE143308.

Transmission electron microscopy

Cells were fixed sliced and mounted (see detailed protocol in supplementary methods) on Formvar/Carbon coated grids. Samples were then stained with uranyl acetate and lead citrate and examined in Jeol 1400 Plus, transmission electron microscope (Jeol, Tokyo, Japan). Images were captured using SIS Megaview III and iTEM the Tem imaging platform (Olympus, Tokyo, Japan). All mice and human measurements and calculations in EM captures, were performed using Fiji open source platform for biological Image analysis. Analysis of patients bone marrow was approved by the IRB committee of Rabin Medical Center (approval 0840-18-RMC).

Oxygen consumption analysis

Oxygen Consumption Rates (OCR) was measured using the Seahorse XF96 Analyzer (Agilent Technologies, Santa Clara, California, USA). Cells were treated and cultured with XF Assay Medium in Seahorse XF96 cell culture plate (30µl) before transferred to the Seahorse XF96 analyzer as detailed in the supplemental methods.

RNAseq

Total RNA was extracted and purified using TRIzolTM Plus RNA Purification Kit (Invitrogen, Carlsbad, California, USA). Library preparation, sequencing data and expression analysis are detailed in the supplemental methods.

Results

Gata2 heterozygosity accelerates leukemia in transgenic ERG mice

We crossed mice transgenic to human *ERG* (Herein tgERG), previously shown to develop AML[18, 20] with Gata2^{het} mice. Time to leukemia and survival significantly shortened (logrank mantel cox test, $p<0.0001$) in tgERG/Gata2^{het} compound mice, compared with tgERG littermates with a Gata2WT background (Fig.1A). To examine the reproducibility of the model we subsequently crossed a Gata2$^{+/L359V}$ knockin mice, provided by SaiJuan Chen, with tgERG mice. GATA2 L359V was previously identified in CML [22]. As with tgERG/Gata2^{het}, tgERG/Gata2$^{+/L359V}$ had an accelerated leukemia and decreased survival time (Fig S1 A, B).

Examination of histopathological sections revealed marked bone marrow infiltration and enlargement of spleens with loss of normal architecture in both tgERG/Gata2^{het} and tgERG leukemic mice (Fig. S1C). Leukemic cells resided within CD45^{dim} gate, and comprised of lineage negative; CD150^{high}; cKit$^{low\text{-}pos}$; Sca1^{neg} cells consistent with Mega-Erythroid Progenitors (MEP) (Fig.1B,C) [23] . Similar findings documented within Gata2$^{+/L359V}$ progeny (Fig S1D). Together the accelerated leukemogenesis upon loss of a Gata2 allele confirms its role as a tumor suppressor.

Transition of Hematopoietic stem cell to proliferating progenitor cells in tgERG/Gata2^{het} preleukemic cells.

Having established the earlier leukemia development in tgERG mice on the background of Gata2 mutation, we were interested to decipher the preleukemic phenotype. We further analyzed differentiation markers on tgERG/Gata2^{het} and tgERG/Gata2^{wt} HSPCs, isolated from 4-6wks non-leukemic bone marrows. To

distinguish between stem and early progenitor cells we used two panels: the first included CD150 and CD48 (Slam molecules), and the second included cKit (CD117), and Sca1[24] . Flow cytometry analysis revealed a significantly higher $CD48^{pos}/CD48^{neg}$ ratio within CD150+ population of tgERG/$Gata2^{het}$ cells (Fig.2A,B). CD48 is an early marker of non-quiescence [25] suggesting increased non-stem progenitors in tgERG/$Gata2^{het}$ mice. Consistent with a greater transition from stem to progenitor cells there was a lower fraction of $Lin^{-}Sca1^{+}cKit^{+}$ cells in the tgERG/$Gata2^{het}$ HSPC s compartment (Fig.2A,C).

We subsequently checked whether associated morphological features can be detected to distinguish tgERG/$Gata2^{het}$ from tgERG/$Gata2^{wt}$ HSPCs. Bone marrow of four preleukemic siblings and two leukemic mice were harvested. Hematopoietic lineage negative (lin-) progenitor cells were selected using magnetic beads and subjected to transmission electron microscopy (TEM). A significant decrease in nuclear to cytoplasmic ratio (NCR) was found in tgERG/$Gata2^{het}$ cells compared with tgERG ($p<0.0001$) (Fig.2D). Decreasing NCR during hematopoiesis typically accompanies the gradual transition of pluripotency to lineage commitment and differentiation [26] and hence is consistent with the dominance of progenitor cells of the tgERG/$Gata2^{het}$ HSPCs compartment.

Early progenitor cells have a greater proliferative capacity than quiescent hematopoietic stem cells [26]. Therefore, we next examined the proliferative potential of tgERG/$Gatat2^{het}$ preleukemic HSPCs. A prominent advantage in colony formation capacity in re-plating methylcellulose assays was observed in tgERG/$Gata2^{het}$ fetal

liver HSPCs compared with counterparts (One-way ANOVA, $p<0.05$) (Fig 3A). We then studied preleukemic HSPCs derived from bone marrow of age matched 4 - 7week-old mice. Cell Trace Proliferation assay demonstrated a significantly higher proliferation index of tgERG/Gata2^{het} HSPCs, compared to ERG/Gata2^{wt} (Fig. 3B). To further identify preleukemic HSPCs sub-populations in tgERG/Gata2^{het}, we conducted 10X single cell RNA sequencing analysis on stem and progenitor cells derived from bone marrow of 4-week-old mice littermates representing the entire genotypic repertoire (WT, Gata2^{het}, tgERG, tgERG/Gata2^{het}). tgERG/Gata2^{het} cells harbored a discrete expression pattern, clustering distinctively apart from tgERG cells, and from the rest two control groups (Fig.3C left). Consistent with the role of ERG and GATA2 in megakaryocytic and erythroid development [3], a functional annotation map, corresponding to expressed key lineage markers, showed that early-erythroid and mid-erythroid were the main lineage modules to contribute to the distinctive tgERG/Gata2^{het} expression profile (Fig 3C right and figure S2A). K-means clustering within groups yielded a cluster of differentially expressed genes, upregulated in tgERG/Gata2^{het} sample (Fig.S2B). This gene set corresponded to Cell Proliferation and Cell Division GO terms. For example, tgERG/Gata2^{het} cells within the erythroid cluster displayed higher expression of Ki67 proliferation marker as well as the mitotic genes Cenpe and Cenpf (Fig. 3D, Fig.S2C). Taken together, immunophenotypic, functional and single cell genomic analysis demonstrate that the loss of WTGata2 allele, endowed tgERG preleukemic cells with an enhanced proliferative and self-renewing hematopoietic progenitor phenotype.

A mitochondrial phenotype in Gata2 mutated mouse and human hematopoietic cells.

To identify potential mechanistic leads that could link Gata2 loss to the HSPCs developmental and proliferative phenotypes, we conducted bulk RNA sequencing experiments in pre-leukemic, and leukemic cells. GSEA [27] showed enrichment of oxidative phosphorylation and mitochondrial metabolism in tgERG/Gata2^{het}. This signature was observed consistently in fetal liver, in preleukemia bone marrow as well as in leukemic cells as shown in Figure 4A and Fig S3. Importantly, oxidative phosphorylation is also a leading gene-set expression signature in tgERG/Gata2$^{+/L359V}$ leukemic cells (Fig. S4A) and in GATA2$^{+/L359V}$ mouse model [28]. To elucidate whether the metabolic signature observed in tgERG/Gata2^{het} mice has relevance to human, we subsequently analyzed expression profiles of AML patients who harbor chromosome 3q26 inversion Inv(3q26)/t(3;3) causing activation of the EVI1 oncogene [29, 30] Intriguingly, oxidative phosphorylation was among the highest ranked pathways to be enriched in *Evi1/GATA2^{MUT}* patients (Fig.4B). Moreover, top ranked gene-sets in ERG/Gata2^{het} mouse model and *Evi1/GATA2^{MUT},* (GSEA, Hallmark cluster)**,** shared common modules, including MYC, and mTOR signaling (S4B). The common expression signatures seen in our mouse models and the human leukemias, suggests that these models are of a general significance to oncogenic driven AML on the background of GATA2 insufficiency state.

To test the functional significance of the mitochondrial gene expression signature, we conducted metabolic analysis. HSPCs, derived from bone marrow of three pairs of preleukemic tgERG/Gata2^{het} and tgERG/Gata2^{wt} mouse siblings were subjected to the Seahorse XF96 analyzer. Basal oxygen consumption rate (OCR) was

significantly higher in tgERG/Gata2^{het} HSPCs (Fig.4C, S5), and a trend toward higher ATP productivity was also found (Fig S5). Interestingly, proton leak was significantly higher in tgERG/Gata2^{het} cells (Fig S5). The proton leak represents ATP-dissociated influx of H+ ions into the mitochondria and can reflect mitochondrial damage [31].

To estimate cellular mitochondrial content, we calculated mtDNA to nuclear DNA (nDNA) copy number ratio using ND1 and r16s as mitochondrial genes and HK2 as a nuclear gene (Fig4D left). Both ND1/HK2 and r16s/HK2 ratios, were significantly higher in tgERG/Gata2^{het} cells (Fig 4D middle and right). Together, these findings suggest tgERG/Gata2^{het} HSPCs to harbor both enhanced oxidative metabolism and mitochondrial abundancy in line with their RNA expression signature.

Disrupted mitochondria in tgERG/Gata2^{het} hematopoietic progenitors

We sought to interrogate whether there are mitochondrial morphological alterations in tgERG/Gata2^{het} cells. Lin- HSPCs of four weeks old preleukemic, and two leukemic, matched age and sex, tgERG and tgERG/Gata2^{het} mice were analyzed by TEM. Cell captures revealed prominent morphological alterations in tgERG/Gata2^{het} mitochondria exhibiting swelling, circular contour and colocalization in clusters. Conversely, tgERG/Gata2^{wt} mitochondria were small, thread shaped, and spread evenly within the cytoplasm (Fig.5A). In addition, the ratio of cumulative mitochondrial area to the cytoplasm of a cell was significantly higher in tgERG/Gata2^{het} (Fig. 5B $p<0.0001$), indicating a higher mitochondrial content (Fig. 5B), consistent with the genomic quantification (Fig 4D).

Ultra-structural characterization of the mitochondrial morphology revealed ill-defined disrupted cristae in tgERG/Gata2^{het}. Some mitochondria were enclosed in a double membraned vacuole, suggesting mitophagy. Conversely, tgERG/Gata2^{wt} mitochondria were elongated and convoluted, with clear electron-dense crista. (Fig 5C, left). Analysis of individual mitochondrion features documented a larger mean area of an individual tgERG/Gata2^{het} mitochondrion. (student t-test, $p<0.0001$) (Fig.5C middle). Additionally, the Aspect Ratio, obtained by dividing the mitochondrial longest axis by the shortest axis, ranging from elongated to round, was significantly lower in tgERG/Gata2^{het} mitochondria, (student t-test, $p<0.0001$) (Fig.5C- right). This feature can be related to differences in mitochondrial dynamics, such as fission preference over fusion, associated with cell division [32] or to increased degradation due to mitochondrial damage. The unique mitochondrial morphology detected in tgERG/Gata2^{het} HSPCs is consistent with the metabolic phenotype. Interestingly, TEM analysis of cells from GATA2 heterozygous mice did not show the same aberrant mitochondrial morphological phenotype as was seen in the tgERG/Gata2^{het} mouse cells (figure S7), although gene expression analysis of progenitor cells from GATAhet demonstrated an upregulation in oxidative phosphorylation gene expression (figure S8). This is in agreement with the minimal hematological phenotype observed in GATA2^{het} mice.

Abnormal mitochondria in hematopoietic progenitors from bone marrow of children with germline GATA2$^{+/R396W}$ mutation. To test whether mitochondrial aberrancy exist in humans with germline mutated GATA2, we examined CD34+ bone marrow cells derived from two siblings of one family harboring GATA2$^{+/R396W}$

mutation (Figure 6A). A 13-year-old male was diagnosed with a germline GATA2 R396W mutation, after presenting with Aplastic Anemia. Genetic analysis of the family revealed the mutation to be transmitted from the asymptomatic father to three of his children: the proband 13-year-old symptomatic son, a 15-year-old asymptomatic daughter and a 7year-old asymptomatic son. A fourth 11-year-old sibling male did not inherit the mutation (Figure 6B).

Complete blood count of the proband patient at presentation demonstrated pancytopenia with severe neutropenia (200 cells/micL), monocytopenia (10 cells/micL) and thrombocytopenia ($24*10^3$/micL). Both asymptomatic carrier siblings displayed normal blood counts with normal cellular indexes. Cytogenetic and somatic gene panel sequencing analysis [7] was normal for both proband and carriers. Bone marrow biopsy the proband revealed remarkable hypocellularity (20% of normal) with myelodysplastic changes. Importantly, albeit normal blood count, the sister's bone marrow demonstrated minimal myelodysplastic changes. No bone marrow examinations were performed the youngest male carrier and the father.

More than 25 CD34 positive bone marrow cells from the patient and the carrier sister were captured using EM (FEI Tecnai SPIRIT, FEI, Eidhoven, Netherlands), analyzed and compared with a healthy donor CD34+ bone marrow cells. A prominent difference in cells general morphology was obvious: while normal control CD34+ cells had a homogenous cytoplasm, and well defined, electron dense mitochondria $GATA2^{+/R396W}$ cells of both sister and the patient had abnormal appearing mitochondria, featured by fragmentation, polymorphism, and disrupted cristae (Fig.6C, D). While quantitative analysis of the mitochondrial morphometrics of the patients CD34+ cells, was difficult to establish due to pronounced cellular disruption and vacuolization, we found the sister's cells to have a significantly

decreased mitochondrial Aspect Ratio, as in the tgERG/Gata2^{het} mice, but also decreased average mitochondrial size, reflecting the ongoing fragmentation state (Fig 6E). Additional finding was a decrease in Nuclear -Cytoplasmic- Ratio, in GATA2$^{+/R396W}$ cells of both the patient's and the sister's cells, compared with normal bone marrow ($p<0.0001$) (Fig S9), similar to what was observed in tgERG/Gata2 ^{het} mouse progenitors. Hence, disrupted mitochondria and reduced NCR characterizes human GATA2 deficiency HSPCs as was observed in the tgERG/Gata2^{het} mouse.

Discussion

Disruptive germline mutations in *GATA2* entail significant risk for developing MDS/AML. Current research has described various effects of GATA2 loss on enhancing the virulence of myeloid and erythroid leukemias [12, 15-17]. Here we focused on interrogating the effect of GATA2 haploinsufficiency on the *preleukemic* phenotype. The tumor suppressive function of Gata2 was uncovered by accelerated ERG driven leukemias in mice with germline Gata2 mutations. We identified enhanced transition of preleukemic HSCs into proliferating early progenitors. These preleukemic progenitors had increased mitochondrial oxidative phosphorylation and increased mitochondrial content with prominent mitochondrial structural aberrations. Strikingly, abnormal mitochondria were detected also in pre-leukemic bone marrow of patients with germline GATA2 mutation including an asymptomatic carrier.

There have been several attempts to unravel the tumor suppressive effect of GATA2 in mouse models by crossing Gata2 mutated mice with mice expressing oncogenic leukemic mutations. Some of these models displayed either complex phenotype or

no malignant transformation[33] while others accelerated the acute leukemic occurrence[16] or altered the leukemic phenotype[17] . For example, Liu P at al. [15] reported enhanced leukemic stem cell phenotype in leukemias arising in a Cbfb-MYH11 knockin/Gata2 heterozygous mouse, but paradoxically latency time to leukemia was extended. Thus, the tumor suppressive effect of GATA2 may depend on the cooperating oncogenes.

Here we exploited tgERG mice to uncover GATA2 tumor suppressive effect focusing on the preleukemic phenotype. ERG is a hematopoietic transcription factor regulating stemness in both normal and leukemic stem cells [34-39]. Indeed, ERG co-regulate HSPCs together with GATA2 as part of a heptad of transcription factors[39]. ERG, GATA2 and TAL1, three of the Heptad's factors, act in a loop regulating erythropoiesis [3]. Strikingly, ERG has been recently shown to be the main driver of leukemias characterized by haploinsufficiency of GATA2 and EVI-1 over expression[21]. This EVI-1 AMLs are highly similar to our mouse model. Interestingly ERG and GATA2 also cooperate in other types of cancers, particularly prostate cancer[40]. Thus, our mouse model is highly relevant as ERG is a likely oncogene mediating leukemia progression of GATA2 germline haploinsuffiency.

The major observation in our study is the presence of marked mitochondrial abnormalities associated with increased expression of oxidative phosphorylation genes and elevated oxygen consumption rates in pre-leukemic Gata2 deficient cells. Interestingly, enhanced expression of genes mediating oxidative phosphorylation were also reported by Yamamoto et al. [16] in murine AML driven by EVi-1 and Gata2 deficiency. Similar to ERG, Evi-1 is also a hematopoietic stem cell transcription factor and an upstream activator of GATA2 [41] . We now show that this mitochondrial

gene expression signature exists also in human EVI-1 leukemias with somatic GATA2 mutations. Similarly activation of oxidative phosphorylation was demonstrated in progression of MPN following loss of LK1/STK11 [42]. Yet here we demonstrate, for the first time, in both the mouse model and in children carrying GATA2 mutation, that the mitochondrial aberrations occur very early, long before progression to frank MDS or leukemia.

These findings may be of general relevance to AML/MDS as prior reports suggested mitochondrial dysfunction and impaired elimination of defective mitochondria (e.g. mitophagy) in MDS/AML[43]. Increased number of mitochondria-containing autophagosomes, and enlarged abnormal mitochondria were also shown in early erythroblasts of MDS patients[44 45]. The described mitochondria phenotype (structural double membrane vacuoles in conjugation with abnormal mitochondrial structure – figure 5) in GATA2het (Fig 6) and tgERG/GATA2het may suggest mitophagy involvement in both the preleukemia state generated by GATA2ht and in the leukemia. MDS patients were reported to have involvement of mitophagy in progression to leukemia. Houwerzijl et al. showed that erythroid precursors from high risk MDS patients have lower mitophagy levels compared with low risk MDS patients. In addition, an MDS mouse model that was generated by deletion of the autophagy protein Atg7, (Vav-Atg7$^{-/-}$) resulted in decreased LSK CD150^{+}CD48^{-} HSCs compartment (which is the population that we describe) and up-regulation of the myeloid leukemia marker CD47 [46].

Analysis of pre-leukemic cells by single cell RNA sequencing revealed that erythroid committed progenitors are the main population to contribute to the differences in expression patterns between tgERG and tgERG/Gata2^{het}. Our observation is similar to recently published findings by Nerlov et al[17] . There, the authors show that Gata2

mutation synergized with CEBPa double mutation to generate a permissive erythroid chromatin state, that promotes leukemogenesis of bilineage acute erythroid /myeloid leukemia. The expansion of highly proliferating erythroid precursors in the tgERG/Gata2^{het} mice was also associated with monocytopenia (Fig S6) which is often observed in human carriers of germline GATA2 mutations[47].

The transition to highly proliferating hematopoietic progenitors was also confirmed by immunophenotyping, in-vitro self-renewal - proliferation assays, TEM analysis of nuclear to cytoplasmic ratio and single cell gene expression analysis. Interestingly, our observation of expanded progenitor compartment (cKit+ lin- and sca1-) and reduced fraction of KLS cells in bone marrow of tgERG/Gata2^{het} preleukemic mice, is also supported by Nerlov's paper, of which GATA2 loss led to expanded progenitors but not KLS compartment [17]. Our observations are reinforced by developmental studies of Gata2 heterozygous mice that demonstrated qualitatively, and quantitatively diminished hematopoietic stem cells accompanied by expansion of hematopoietic progenitors [1, 13]. Thus, GATA2 haploinsufficiency may create a premature aging phenotype of HSPCs characterized by increased transition to progenitors coupled with increased susceptibility to oncogenic transformation.

The transition from quiescence to proliferative preleukemic progenitors may also partially explain the mitochondrial phenotype in tgERG/Gata2^{het}. This transition generates a steep increase in energetic demands, and hence, oxidative phosphorylation preference over glycolysis, mitochondrial fission/ fragmentation, and a flux of reactive oxygen species[48]. It is possible that the loss of GATA2 as a stem cell gate keeper causes transition from quiescence into a proliferative state associated with increased mitochondrial mass and activity. If unrestricted cycling is

ongoing, the cellular scavenging machinery may fail to sufficiently neutralize genotoxic molecules. Abnormal mitochondrial dynamics may have a genuine effect on GATA2 deficiency leukemogenic evolvement and may be also a vulnerability that could be therapeutically targeted for prevention and treatment of these leukemias. While several drugs have been suggested to lower leukemia mitochondrial activity [reviewed in [49]], replacement of bone marrow transplantation by chronic drug therapy suppressing the preleukemic phenotype is a major challenge. This represents one of the leading “unmet needs” in the management of cancer predisposition syndromes: can we alter their course by pharmacological approach?

References:

1. Rodrigues NP, Janzen V, Forkert R, et al. Haploinsufficiency of GATA-2 perturbs adult hematopoietic stem-cell homeostasis. Blood. 2005;106(2):477-484.

2. Tsai FY, Keller G, Kuo FC, et al. An early haematopoietic defect in mice lacking the transcription factor GATA-2. Nature. 1994;371(6494):221-226.

3. Thoms JAI, Truong P, Subramanian S, et al. Disruption of a GATA2-TAL1-ERG regulatory circuit promotes erythroid transition in healthy and leukemic stem cells. Blood. 2021;138(16):1441-1455.

4. Menendez-Gonzalez JB, Vukovic M, Abdelfattah A, et al. Gata2 as a Crucial Regulator of Stem Cells in Adult Hematopoiesis and Acute Myeloid Leukemia. Stem Cell Reports. 2019;13(2):291-306.

5. Chaytor L, Simcock M, Nakjang S, et al. The Pioneering Role of GATA2 in Androgen Receptor Variant Regulation Is Controlled by Bromodomain and Extraterminal Proteins in Castrate-Resistant Prostate Cancer. Mol Cancer Res. 2019;17(6):1264-1278.

6. Kennedy JA, Ebert BL. Clinical Implications of Genetic Mutations in Myelodysplastic Syndrome. J Clin Oncol. 2017;35(9):968-974.

7. Noy-Lotan S, Krasnov T, Dgany O, et al. Incorporation of somatic panels for the detection of haematopoietic transformation in children and young adults with leukaemia predisposition syndromes and with acquired cytopenias. Br J Haematol. 2021;193(3):570-580.

8. Donadieu J, Lamant M, Fieschi C, et al. Natural history of GATA2 deficiency in a survey of 79 French and Belgian patients. Haematologica. 2018;103(8):1278-1287.

9. Al Seraihi AF, Rio-Machin A, Tawana K, et al. GATA2 monoallelic expression underlies reduced penetrance in inherited GATA2-mutated MDS/AML. Leukemia. 2018;32(11):2502-2507.

10. Wlodarski MW, Hirabayashi S, Pastor V, et al. Prevalence, clinical characteristics, and prognosis of GATA2-related myelodysplastic syndromes in children and adolescents. Blood. 2016;127(11):1387-1397; quiz 1518.

11. Churpek JE, Bresnick EH. Transcription factor mutations as a cause of familial myeloid neoplasms. J Clin Invest. 2019;129(2):476-488.

12. Sahoo SS, Kozyra EJ, Wlodarski MW. Germline predisposition in myeloid neoplasms: Unique genetic and clinical features of GATA2 deficiency and SAMD9/SAMD9L syndromes. Best Pract Res Clin Haematol. 2020;33(3):101197.

13. de Pater E, Kaimakis P, Vink CS, et al. Gata2 is required for HSC generation and survival. J Exp Med. 2013;210(13):2843-2850.

14. Dzierzak E, Bigas A. Blood Development: Hematopoietic Stem Cell Dependence and Independence. Cell Stem Cell. 2018;22(5):639-651.

15. Saida S, Zhen T, Kim E, et al. Gata2 deficiency delays leukemogenesis while contributing to aggressive leukemia phenotype in Cbfb-MYH11 knockin mice. Leukemia. 2020;34(3):759-770.

16. Katayama S, Suzuki M, Yamaoka A, et al. GATA2 haploinsufficiency accelerates EVI1-driven leukemogenesis. Blood. 2017;130(7):908-919.

17. Di Genua C, Valletta S, Buono M, et al. C/EBPalpha and GATA-2 Mutations Induce Bilineage Acute Erythroid Leukemia through Transformation of a Neomorphic Neutrophil-Erythroid Progenitor. Cancer Cell. 2020;37(5):690-704.e8.

18. Goldberg L, Tijssen MR, Birger Y, et al. Genome-scale expression and transcription factor binding profiles reveal therapeutic targets in transgenic ERG myeloid leukemia. Blood. 2013;122(15):2694-2703.

19. Taoudi S, Bee T, Hilton A, et al. ERG dependence distinguishes developmental control of hematopoietic stem cell maintenance from hematopoietic specification. Genes Dev. 2011;25(3):251-262.

20. Birger Y, Goldberg L, Chlon TM, et al. Perturbation of fetal hematopoiesis in a mouse model of Down syndrome's transient myeloproliferative disorder. Blood. 2013;122(6):988-998.

21. Schmoellerl J, Barbosa IAM, Minnich M, et al. EVI1 drives leukemogenesis through aberrant ERG activation. Blood. 2022 Sep 12. [Epub ahead of print]

22. Zhang SJ, Ma LY, Huang QH, et al. Gain-of-function mutation of GATA-2 in acute myeloid transformation of chronic myeloid leukemia. Proc Natl Acad Sci U S A. 2008;105(6):2076-2081.

23. Pronk CJ, Rossi DJ, Mansson R, et al. Elucidation of the phenotypic, functional, and molecular topography of a myeloerythroid progenitor cell hierarchy. Cell Stem Cell. 2007;1(4):428-442.

24. Boles KS, Nakajima H, Colonna M, et al. Molecular characterization of a novel human natural killer cell receptor homologous to mouse 2B4. Tissue Antigens. 1999;54(1):27-34.

25. Oguro H, Ding L, Morrison SJ. SLAM family markers resolve functionally distinct subpopulations of hematopoietic stem cells and multipotent progenitors. Cell Stem Cell. 2013;13(1):102-116.

26. Passegue E, Wagers AJ, Giuriato S, Anderson WC, Weissman IL. Global analysis of proliferation and cell cycle gene expression in the regulation of hematopoietic stem and progenitor cell fates. J Exp Med. 2005;202(11):1599-1611.

27. Subramanian A, Tamayo P, Mootha VK, et al. Gene set enrichment analysis: a knowledge-based approach for interpreting genome-wide expression profiles. Proc Natl Acad Sci U S A. 2005;102(43):15545-15550.

28. Fu YK, Tan Y, Wu B, et al. Gata2-L359V impairs primitive and definitive hematopoiesis and blocks cell differentiation in murine chronic myelogenous leukemia model. Cell Death Dis. 2021;12(6):568.

29. Groschel S, Sanders MA, Hoogenboezem R, et al. A single oncogenic enhancer rearrangement causes concomitant EVI1 and GATA2 deregulation in leukemia. Cell. 2014;157(2):369-381.

30. Yamazaki H, Suzuki M, Otsuki A, et al. A remote GATA2 hematopoietic enhancer drives leukemogenesis in inv(3)(q21;q26) by activating EVI1 expression. Cancer Cell. 2014;25(4):415-427.

31. Divakaruni AS, Paradyse A, Ferrick DA, Murphy AN, Jastroch M. Analysis and interpretation of microplate-based oxygen consumption and pH data. Methods Enzymol. 2014;547(309-354.

32. Khacho M, Clark A, Svoboda DS, et al. Mitochondrial Dynamics Impacts Stem Cell Identity and Fate Decisions by Regulating a Nuclear Transcriptional Program. Cell Stem Cell. 2016;19(2):232-247.

33. Shimizu R, Yamamoto M. Quantitative and qualitative impairments in GATA2 and myeloid neoplasms. IUBMB Life. 2020;72(1):142-150.

34. Loughran SJ, Kruse EA, Hacking DF, et al. The transcription factor Erg is essential for definitive hematopoiesis and the function of adult hematopoietic stem cells. Nat Immunol. 2008;9(7):810-819.

35. Lacadie SA, Zon LI. The ERGonomics of hematopoietic stem cell self-renewal. Genes Dev. 2011;25(4):289-293.

36. Knudsen KJ, Rehn M, Hasemann MS, et al. ERG promotes the maintenance of hematopoietic stem cells by restricting their differentiation. Genes Dev. 2015;29(18):1915-1929.

37. Salek-Ardakani S, Smooha G, de Boer J, et al. ERG is a megakaryocytic oncogene. Cancer Res. 2009;69(11):4665-4673.

38. Yassin M, Aqaqe N, Yassin AA, et al. A novel method for detecting the cellular stemness state in normal and leukemic human hematopoietic cells can predict disease outcome and drug sensitivity. Leukemia. 2019;33(8):2061-2077.

39. Diffner E, Beck D, Gudgin E, et al. Activity of a heptad of transcription factors is associated with stem cell programs and clinical outcome in acute myeloid leukemia. Blood. 2013;121(12):2289-2300.

40. Buscheck F, Zub M, Heumann A, et al. The independent prognostic impact of the GATA2 pioneering factor is restricted to ERG-negative prostate cancer. Tumour Biol. 2019;41(7):1010428318824815.

41. Sato T, Goyama S, Nitta E, et al. Evi-1 promotes para-aortic splanchnopleural hematopoiesis through up-regulation of GATA-2 and repression of TGF-b signaling. Cancer Sci. 2008;99(7):1407-1413.

42. Marinaccio C, Suraneni P, Celik H, et al. LKB1/STK11 Is a Tumor Suppressor in the Progression of Myeloproliferative Neoplasms. Cancer Discov. 2021;11(6):1398-1410.

43. Joshi A, Kundu M. Mitophagy in hematopoietic stem cells: the case for exploration. Autophagy. 2013;9(11):1737-1749.

44. Watson AS, Mortensen M, Simon AK. Autophagy in the pathogenesis of myelodysplastic syndrome and acute myeloid leukemia. Cell Cycle. 2011;10(11):1719-1725.

45. Houwerzijl EJ, Pol HW, Blom NR, van der Want JJ, de Wolf JT, Vellenga E. Erythroid precursors from patients with low-risk myelodysplasia demonstrate ultrastructural features of enhanced autophagy of mitochondria. Leukemia. 2009;23(5):886-891.

46. Mortensen M, Soilleux EJ, Djordjevic G, et al. The autophagy protein Atg7 is essential for hematopoietic stem cell maintenance. J Exp Med. 2011;208(3):455-467.

47. Bigley V, Collin M. Dendritic cell, monocyte, B and NK lymphoid deficiency defines the lost lineages of a new GATA-2 dependent myelodysplastic syndrome. Haematologica. 2011;96(8):1081-1083.

48. Filippi MD, Ghaffari S. Mitochondria in the maintenance of hematopoietic stem cells: new perspectives and opportunities. Blood. 2019;133(18):1943-1952.

49. Egan G, Khan DH, Lee JB, Mirali S, Zhang L, Schimmer AD. Mitochondrial and Metabolic Pathways Regulate Nuclear Gene Expression to Control Differentiation, Stem Cell Function, and Immune Response in Leukemia. Cancer Discov. 2021;11(5):1052-1066.

50. Valente AJ, Maddalena LA, Robb EL, Moradi F, Stuart JA. A simple ImageJ macro tool for analyzing mitochondrial network morphology in mammalian cell culture. Acta Histochem. 2017;119(3):315-326.

Figure legends

Figure 1. Accelerated leukemia and reduced survival in Gata2-haploinsufficient tgERG mice **A. Survival curve showing** reduced survival (log rank Mantel-Cox test, $p<0.0001$) in ERG/Gata2^{het} (blue, n=43) mice compared to tgERG/Gata2^{wt} (herein ERG , red, n=59) littermates. **B**. Flow cytometery plot depicting immune phenotyping of Lin (-) leukemia cells. Upper panel: cell scatter. Lower panel: Lin (-) HSPCs, residing in a CD45^{dim} gate, expressing CD150^{high}, and cKit$^{low/+}$. Leukemic population is circled. **C.** Dot plots of CD45^{dim}, CD150, and cKit showing no differences in proportions of expressed membranal markers between the two leukemias (lines represent mean values, $p<0.05$, Student T-test). Sp. - spleen BM.-bone marrow

Figure 2. Progenitors expansion within tgERG/Gata2^{het} pre-leukemic HSPC compartment

Lin- cells were immunophenotyped for progenitor compartments according to SLAM markers(B) and classical LSK markers (C)

A A diagram illustrating different stages of progenitors by CD150 and CD48 (slam1, slam2, respectively) combined expression and classical LSK differentiation. **B** Left - Representative flow cytometry graphs demonstrating CD48 and CD150 gating approach. Right- dot graph summarizing 6 experiments (student t-test, n=6, *$p<0.05$). **C**. Left- Representative cytometry plots of 2 experiments. Right - dot graph depicting comparison of LSKs proportions (student t-test, n=7, *$p<0.05$). **D**. Transmission electron microscopy images (TEM) was used to calculate nuclear to

cytoplasmic ratio of leukemic and preleukemic cells. Left - Demarcation of cytoplasm (light blue) and nuclei (dark blue). Cells were derived from two pre-leukemic mice, and one leukemic mouse for either tgERG (left cells grid), and tgERG/Gata2^{het} (right cells grid). 1:12 000 magnification scale, calibrated by Fiji tool (1µm = 124 pixel). Right- A decreased nuclear to cytoplasmic ratio (NCR) was found in tgERG/Gata2^{het} cells (student t-test, p<0.0001)**.**

HPC-hematopoietic progenitor cells, **HSC-** hematopoietic stem cells**, MPP-** multipotential progenitors.

Figure 3. Proliferative phenotype in ERG/Gata2^{het} pre-leukemia progenitor cells

A. Enhanced proliferation and re-plating capacity of tgERG/Gata2^{het} fetal livers HSPCs. Top: replanting illustration. Bottom, bar graph summing 3 independent re-plating assays of E14.5 fetal livers (n=6-8 / genotypic group, Oneway ANOVA and unpaired student t-test, error bars - SEM, *p < 0.05, **p < 0.01, ***p<0.0001.). **B.** tgERG/Gata2^{het} bone marrow HSPC's have a higher proliferation index in CFSE assay. Representative histograms of two CFSE dilutional courses are portrayed (left), showing tgERG and tgERG/Gata2^{het} at 0, 72, and 96 hours from staining. Right- a summary of six independent experiments (paired student t-test p<0.05). **C**. Two-dimensional projection plot of Metacell model on 10X single cell analysis of preleukemic lineage negative progenitors showing (Top): tgERG/Gata2^{het} cells clustered distinctively (green zone) from tgERG (red zone), and from Gata2^{het} (light blue), and WT (purple). Light blue line delineates the area were tgERG and tgERG/Gata2^{het} clustered differentially.(Bottom): functional annotation plot of Meta-cells by expression of key lineage markers, depicting Early erythroid (pink) and Mid erythroid (red) modules, are dominantly expressed in both tgERG/Gata2^{het} and tgERG expression profiles**.** This is shown by projecting the genotype expression

map (top) over the lineage expression map(bottom). Thus, expression differences between tgERG and tgERG/Gata2het, mostly occur in early and mid-erythroid. An additional line, roughly separates early from mid erythroid program zones. **D.** Ki67, Cenpf and Cenpe (mitosis related genes) expression projections on metacell plot are illustrated, alongside with the global expression scheme of tgERG/Gata2^{het} (upper left). The genes are highly expressed in tgERG/Gata2^{het} territory. Dark blue- high expression, yellow-white- low expression.

Figure 4. Enhanced oxidative phosphorylation in Gata2 mutated leukemias. **A.** GSEA plots depicting 'Oxidative Phosphorylation pathway enrichment in tgERG/Gata2^{het} RNAseq expression profiles, comparing with tgERG/Gata2^{wt}. **B.** 'Oxidative Phosphorylation signature is enriched in human Inv(3)/GATA2-mutated AML leukemia cells expression profiles, as portrayed in GSEA plot. **C.** Basal oxygen consumption rate (OCR) is significantly higher in tgERG/Gata2^{het} HSPCs preleukemia cells, SeaHorse XF assay ($p<0.05$, student t-test 1 out of 3 independent experiments. Arrows- time of intervention). **D.** Left- illustration of mouse mitochondrial DNA with the genes ND1 and r16s marked. Right- bar graphs depicting qPCR quantitation of mitochondrial to nuclear DNA ratio that was calculated using ND1 and r16s. tgERG/Gata2^{het} HSPCs harbor a higher ratio of mitochondrial/nuclear DNA copy number (n=3-4, nuclear reference gene - HK2, $p<0.05$, student t-test)

Figure 5. Mitochondrial structural aberrations in tgERG/Gata2^{het} preleukemic hematopoietic progenitors. A. tgERG/Gata2^{het} hematopoietic lineage negative progenitors exhibit mitochondrial disruptions, as shown in Transmission electrons microscopy captures imaging, both in pre-leukemia and leukemia cells. Left- tgERG

HSPCs mitochondria are spread within cytoplasm. Right - tgERG/Gata2^{het} mitochondria are swollen, rounded, and tend to group in clusters. Upper- unprocessed capture, lower - ImageJ processed view. mitochondria- light blue, nuclei- beige. Magnification scale 1:12 000. **B.** Total mitochondrial surface per cell is increased in tgERG/Gata2^{het} hematopoietic progenitors. Representative illustration by ImageJ (left), and a dot bar graph (right) (n= 25-31 cells per genotype, unpaired student t-test, $p<0.0001$). **C.** Left- Ultra-structurally- mitochondria of tgERG/Gata2^{wt} progenitors (tgERG) are elongated, torturous, and display electron dense, clearly defined cristae (up)**.** tgERG/Gata2^{het} progenitors display spherical, swollen mitochondria and distorted, blurred cristae (down). (Magnification 1: 20 000 ; 1:50 000 respectively; yellow quadrangles show magnification view of mitochondrial structure). Middle- Dot plot depicting Mean surface area of an individual mitochondrion is higher in tgERG/Gata2^{het} progenitors, (unpaired student t- test, $p<0.0001$). Right - Dot plot depicting Mitochondrial aspect ratio, (representing longest to shortest axis ratio), is lower in tgERG/Gata2^{het} (unpaired student T- test, $p<0.0001$), indicating spherical contour, instead of thread shape (calculated by Fiji NIH program[50]).

Figure 6. Mitochondrial aberrations in Human GATA2+/R396W mutated hematopoietic progenitors. A. Schematic illustration of the GATA2 germline R396W substitution mutation switching Arginine to Tryptophan. **B.** A family pedigree scheme of the 13-year-old GATA2+/R396W patient (arrow) diagnosed and treated in our hospital. (circle- female, quadrangle- male) **C.** Transmission electrons microscopy captures of CD34+ bone marrow cells show fragmented mitochondria (top quadrangles- original capture) designated by pseudo-color light green (large quadrangles). Fragmentation is shown in carrier sister, and the patient (left and

middle, respectively) compared to normal sized and contour mitochondria of donor CD34+ bone marrow cells (right). (scale 1:4800 to 1:6800, Fiji NIH program[51]). **D.** Ultrastructure of mitochondria - fragmentation and disruption of cristae in carrier and sister (left and middle captures, respectively), and organized well-defined and electron-dense cristae in control cells mitochondria. (right capture) (FEI Tecnai SPIRIT, Eindhoven, Netherlands scale 1:6 800 -1:9 300). **E.** Mean surface area of an individual mitochondrion is lower (left) in $GATA2^{+/R396W}$ carrier (sister) CD34+ HSPCs compared with normal control. (unpaired student t- test, $p<0.0001$). Mitochondrial aspect ratio (right), (representing longest to shortest axis ratio), is lower in $GATA2^{+/R396W}$ carrier (unpaired student t- test, $p<0.0001$), which reflects fragmented formation instead of thread shape [calculated by Fiji NIH program[50]].

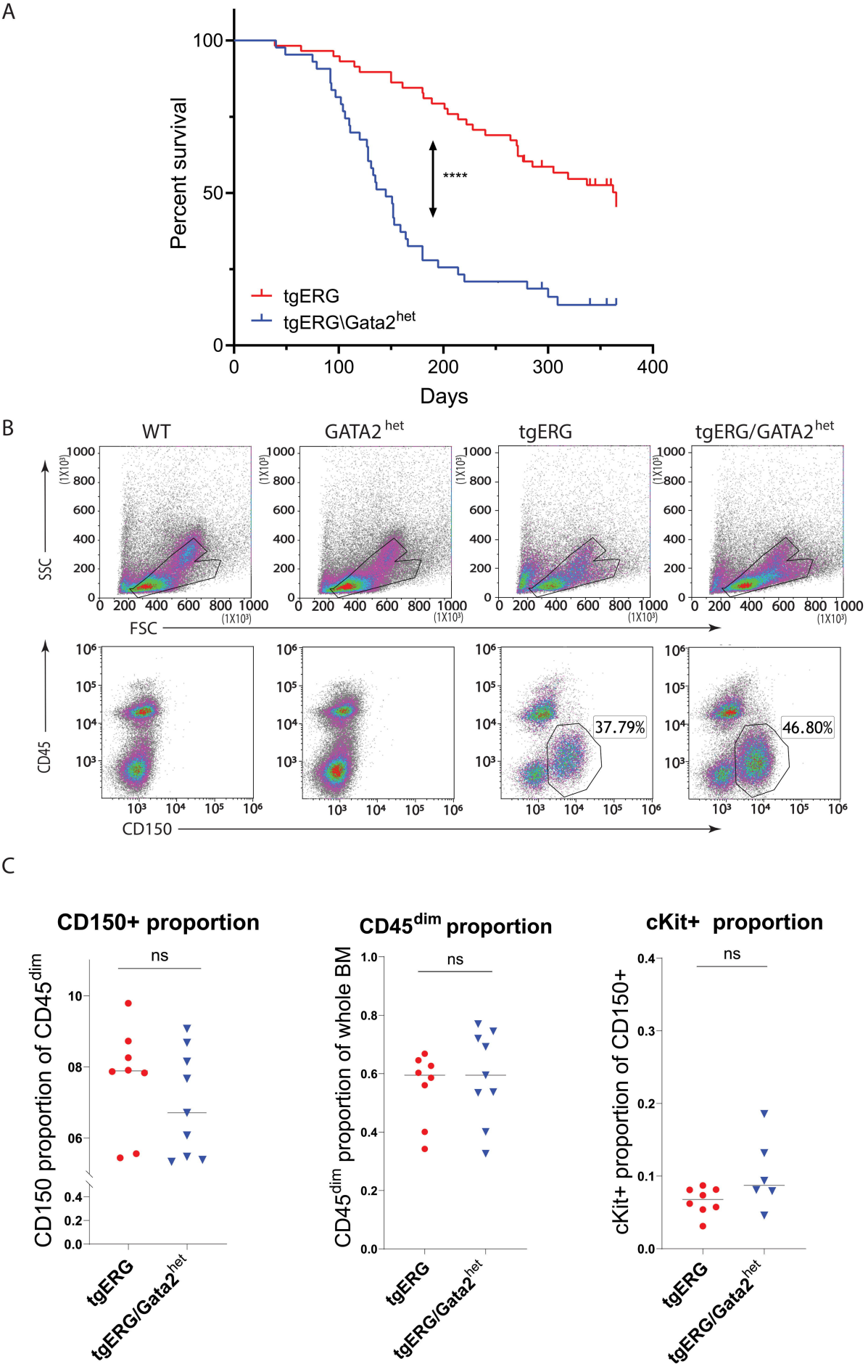
A
Percent survival
100
50
0
****
tgERG
tgERG\Gata2het
0
100
200
300
400
Days
B
WT
GATA2 het
tgERG
tgERG/GATA2het
SSC
FSC
CD45
CD150
37.79%
46.80%
C
CD150+ proportion
CD150 proportion of CD45dim
ns
tgERG
tgERG/Gata2het
CD45dim proportion
CD45dim proportion of whole BM
cKit+ proportion
cKit+ proportion of CD150+

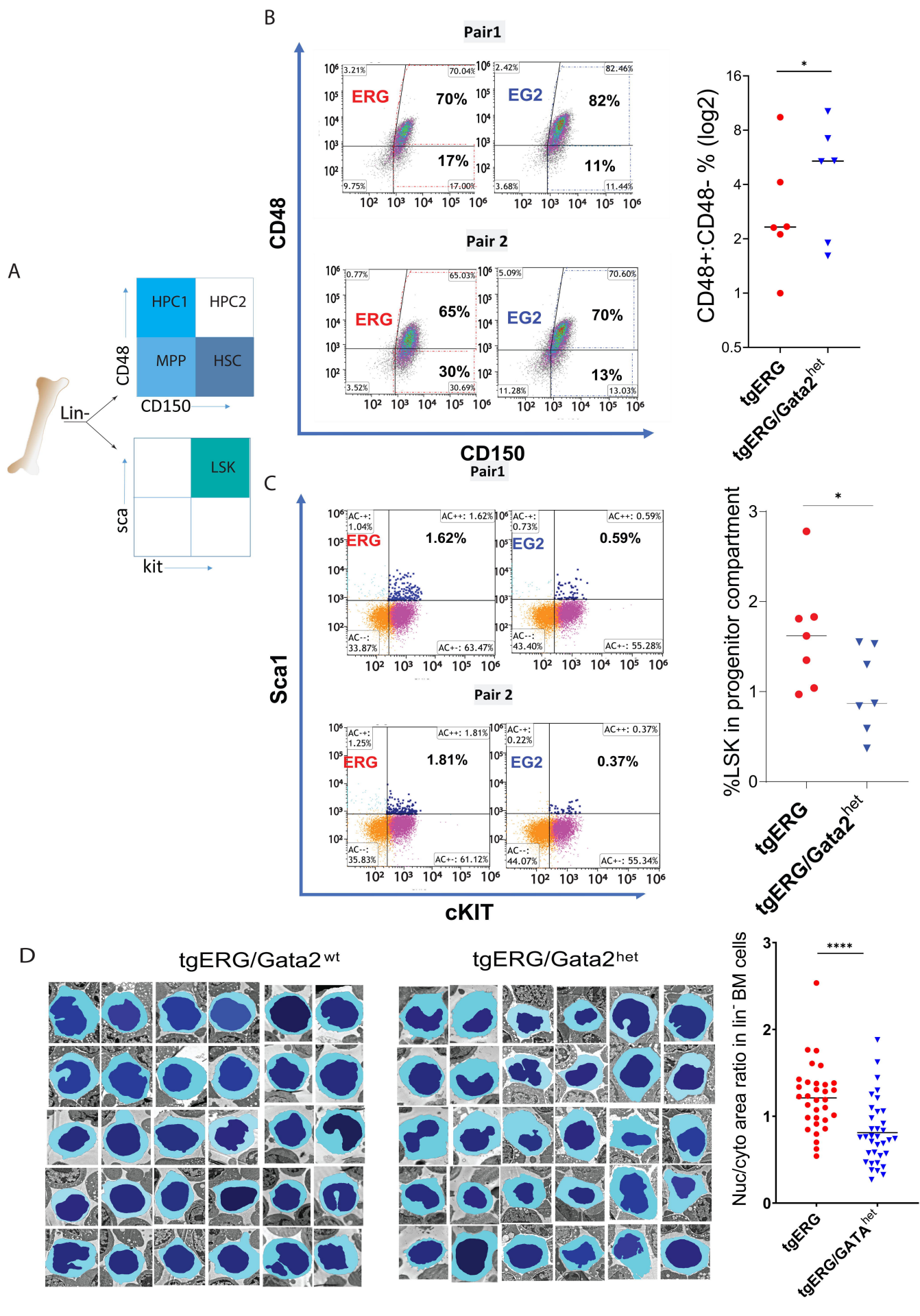
A
HPC1
HPC2
MPP
HSC
CD48
CD150
Lin-
LSK
sca
kit
B
Pair1
ERG
70%
17%
3.21%
70.04%
9.75%
17.00%
EG2
82%
11%
2.42%
82.46%
3.68%
11.44%
Pair 2
ERG
65%
30%
0.77%
65.03%
3.52%
30.69%
EG2
70%
13%
5.09%
70.60%
11.28%
13.03%
CD48
CD150
CD48+:CD48- % (log2)
*
tgERG
tgERG/Gata2het
C
Pair1
ERG
1.62%
AC++: 1.62%
1.04%
33.87%
63.47%
EG2
0.59%
AC++: 0.59%
0.73%
43.40%
55.28%
Pair 2
ERG
1.81%
AC++: 1.81%
1.25%
35.83%
61.12%
EG2
0.37%
AC++: 0.37%
0.22%
44.07%
55.34%
Sca1
cKIT
%LSK in progenitor compartment
*
tgERG
tgERG/Gata2het
D
tgERG/Gata2wt
tgERG/Gata2het
Nuc/cyto area ratio in lin- BM cells
****
tgERG
tgERG/GATAhet

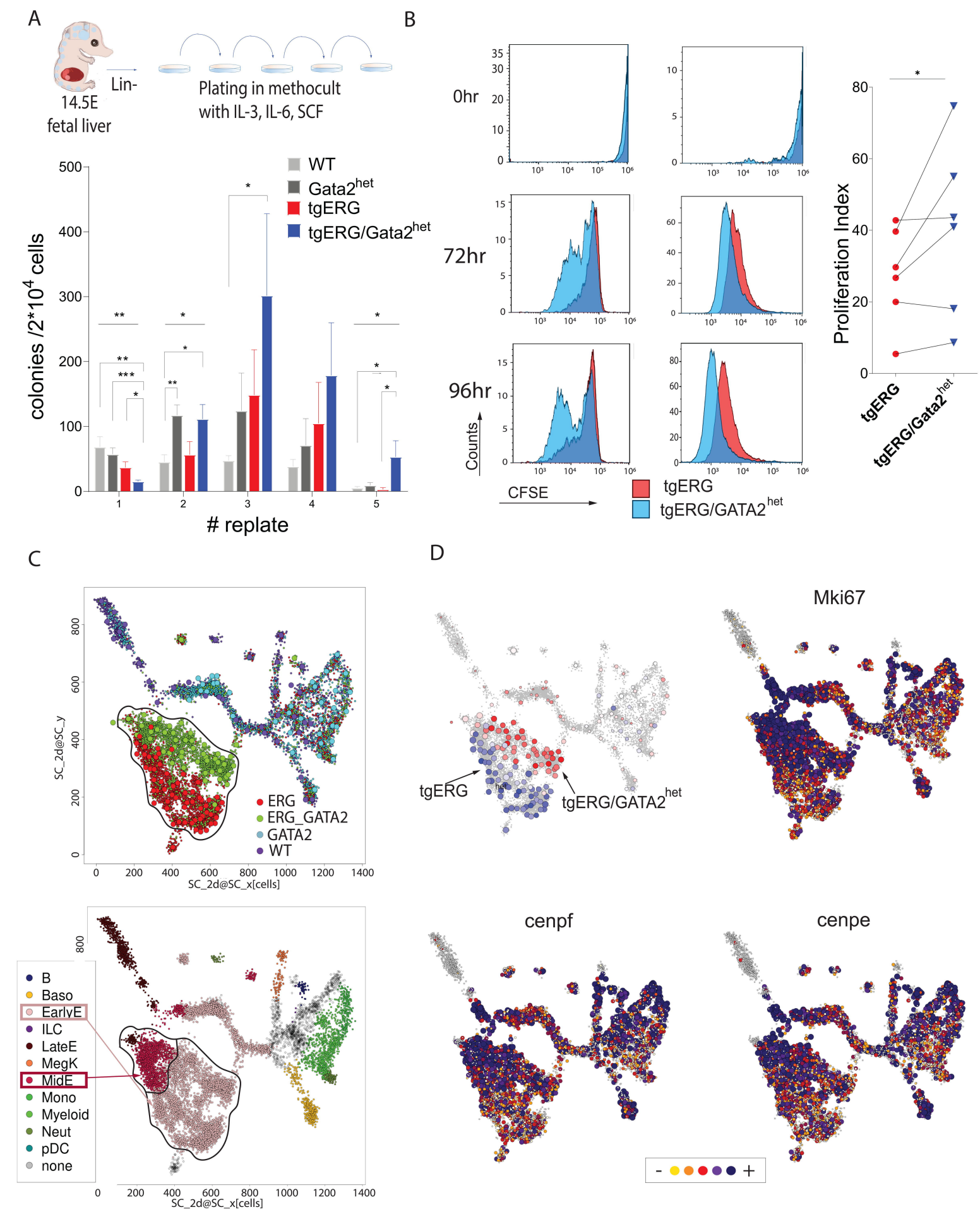
A
14.5E
fetal liver
Lin-
Plating in methocult
with IL-3, IL-6, SCF
WT
Gata2het
tgERG
tgERG/Gata2het
colonies /2*10^4 cells
replate
B
0hr
72hr
96hr
Counts
CFSE
tgERG
tgERG/GATA2het
Proliferation Index
C
SC_2d@SC_y
SC_2d@SC_x[cells]
ERG
ERG_GATA2
GATA2
WT
B
Baso
EarlyE
ILC
LateE
MegK
MidE
Mono
Myeloid
Neut
pDC
none
D
tgERG
tgERG/GATA2het
Mki67
cenpf
cenpe
-
+

A

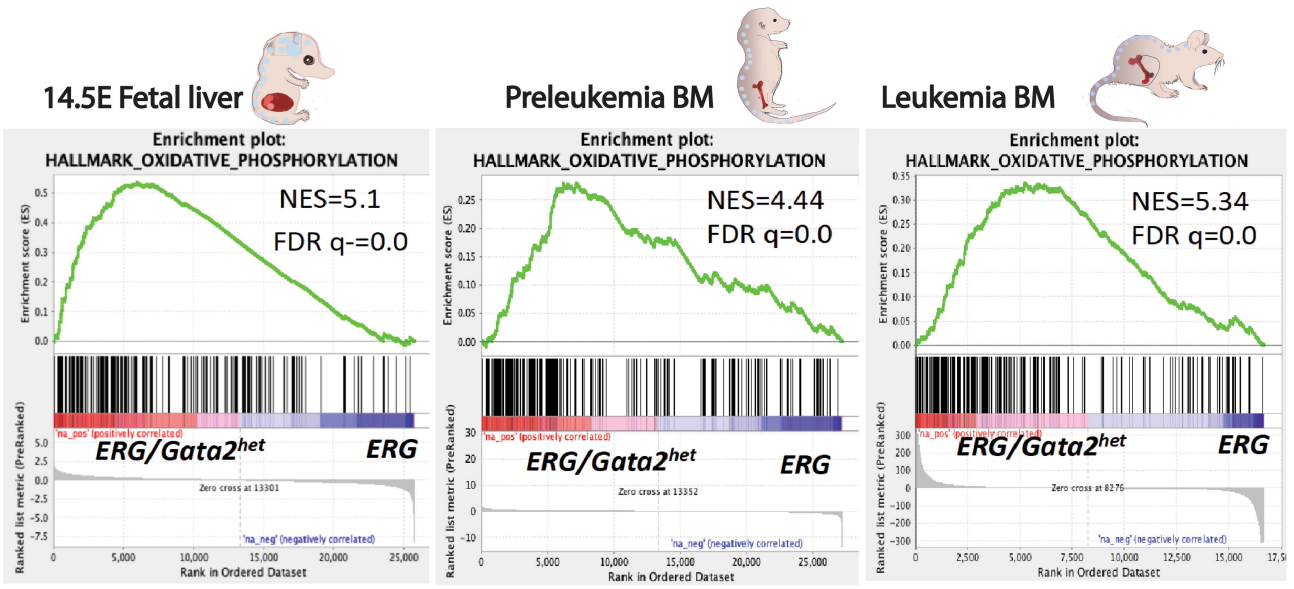
14.5E Fetal liver
Preleukemia BM
Leukemia BM
Enrichment plot:
HALLMARK_OXIDATIVE_PHOSPHORYLATION
NES=5.1
FDR q-=0.0
ERG/Gata2het
ERG
Zero cross at 13301
Rank in Ordered Dataset
Enrichment plot:
HALLMARK_OXIDATIVE_PHOSPHORYLATION
NES=4.44
FDR q=0.0
ERG/Gata2het
ERG
Zero cross at 13352
Rank in Ordered Dataset
Enrichment plot:
HALLMARK_OXIDATIVE_PHOSPHORYLATION
NES=5.34
FDR q=0.0
ERG/Gata2het
ERG
Zero cross at 8276
Rank in Ordered Dataset

B

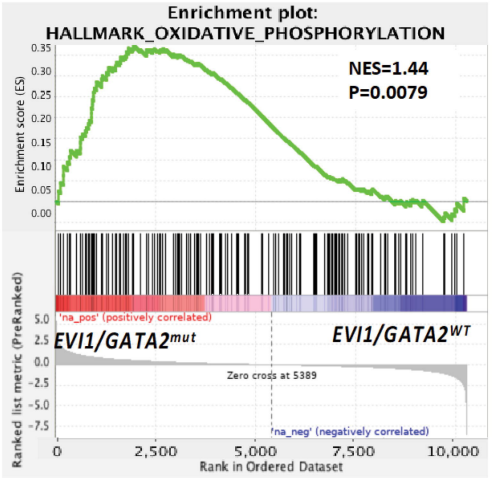
Human Leukemia BM
Enrichment plot:
HALLMARK_OXIDATIVE_PHOSPHORYLATION
NES=1.44
P=0.0079
EVI1/GATA2mut
EVI1/GATA2WT
Zero cross at 5389
Rank in Ordered Dataset

C

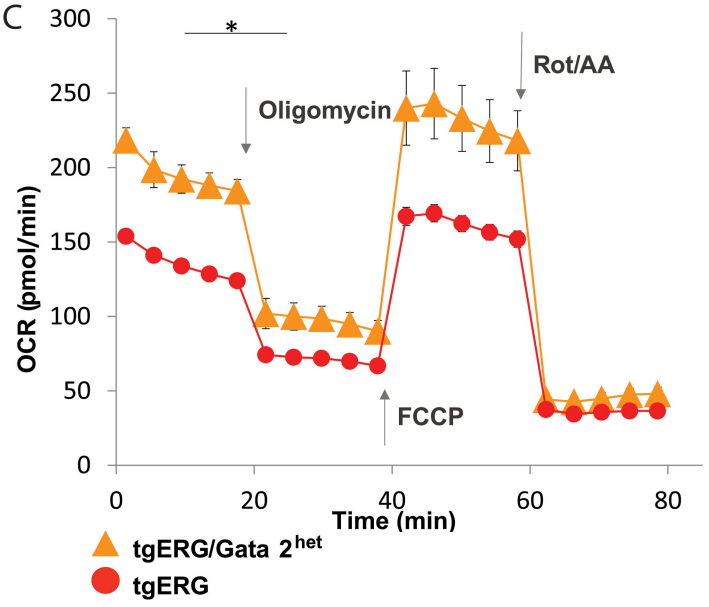
*
Rot/AA
Oligomycin
FCCP
OCR (pmol/min)
Time (min)
tgERG/Gata 2het
tgERG

D

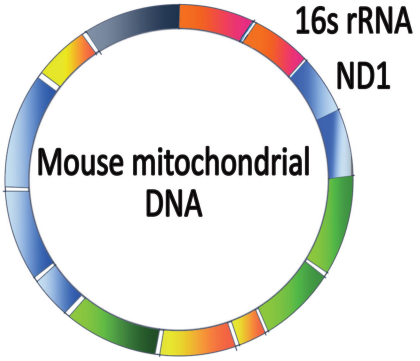
16s rRNA
ND1
Mouse mitochondrial DNA

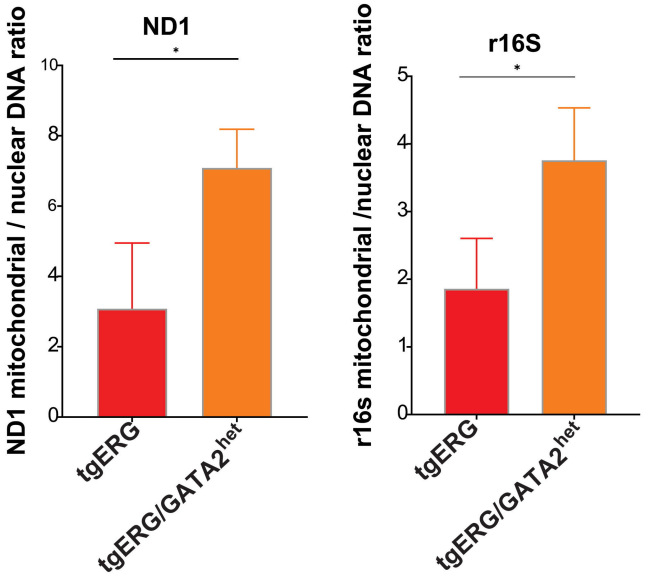
ND1
*
ND1 mitochondrial / nuclear DNA ratio
tgERG
tgERG/GATA2het
r16S
*
r16s mitochondrial /nuclear DNA ratio
tgERG
tgERG/GATA2het

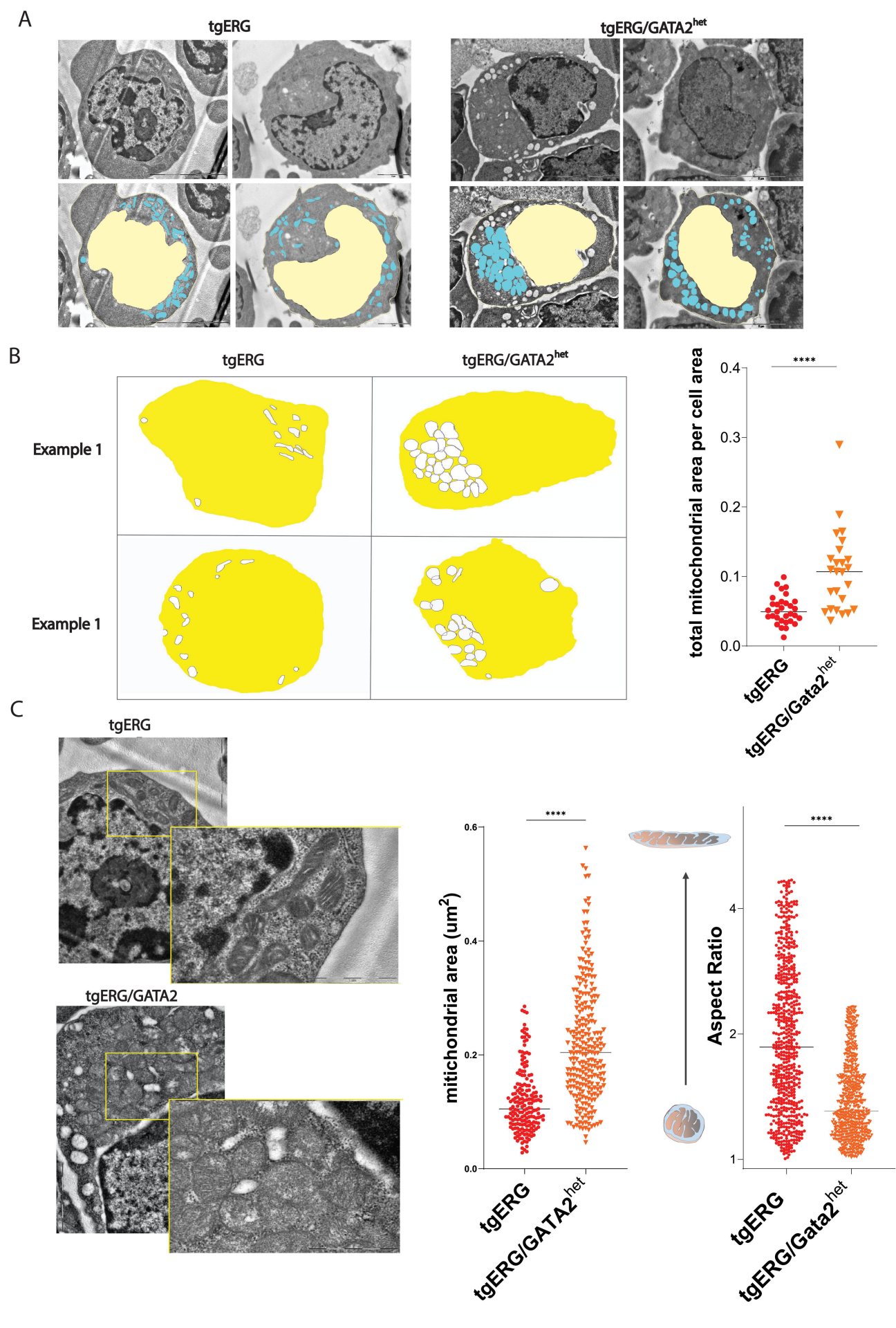
A
tgERG
tgERG/GATA2het
B
tgERG
tgERG/GATA2het
Example 1
Example 1
total mitochondrial area per cell area
****
0.4
0.3
0.2
0.1
0.0
tgERG
tgERG/Gata2het
C
tgERG
tgERG/GATA2
mitichondrial area (um2)
****
0.6
0.4
0.2
0.0
tgERG
tgERG/GATA2het
Aspect Ratio
****
4
2
1
tgERG
tgERG/Gata2het

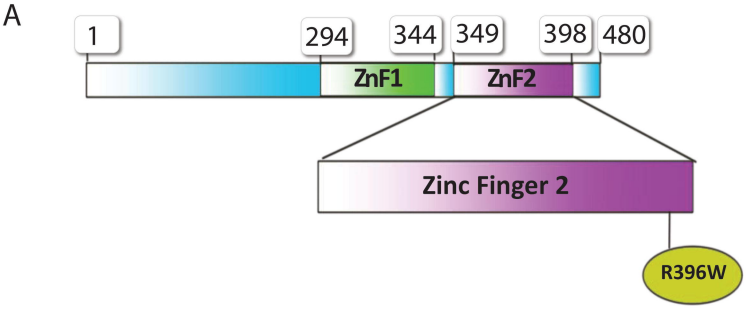
A
1
294
344
349
398
480
ZnF1
ZnF2
Zinc Finger 2
R396W

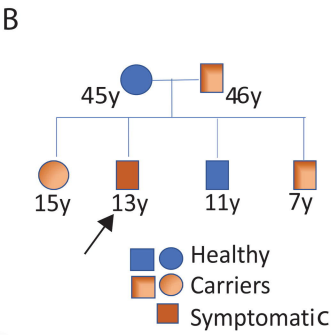
B
45y
46y
15y
13y
11y
7y
Healthy
Carriers
Symptomatic

C

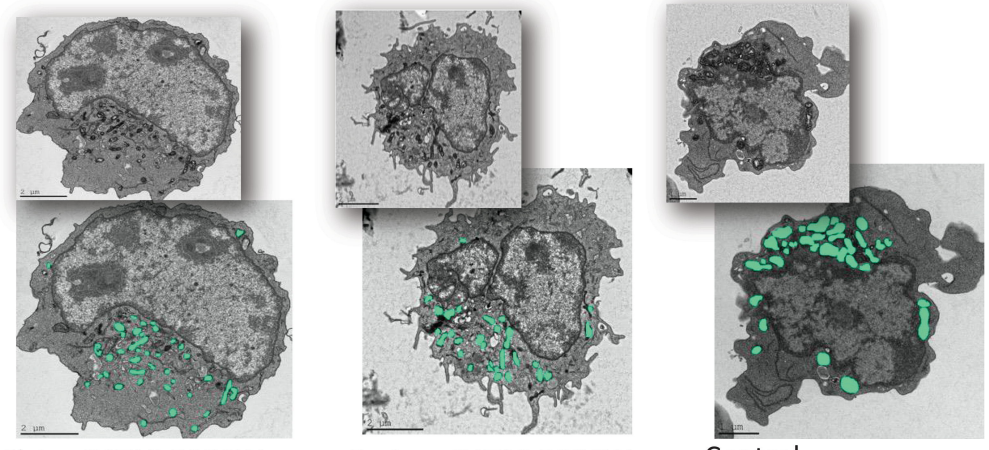
Sister GATA2 R396W
Patient GATA2 R396W
Control

D

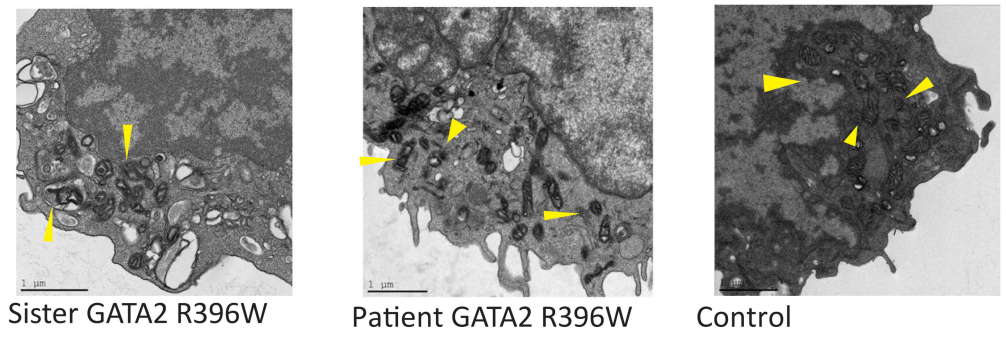
Sister GATA2 R396W
Patient GATA2 R396W
Control

E

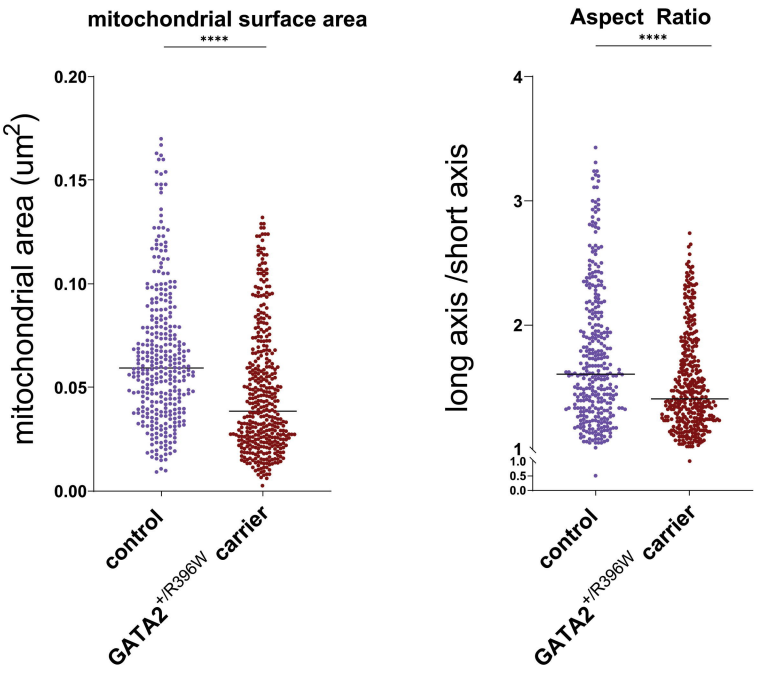
mitochondrial surface area
****
mitochondrial area (um2)
0.20
0.15
0.10
0.05
0.00
control
GATA2+/R396W carrier
Aspect Ratio
****
long axis /short axis
4
3
2
1
1.0
0.5
0.0
control
GATA2+/R396W carrier

Supplemental Data

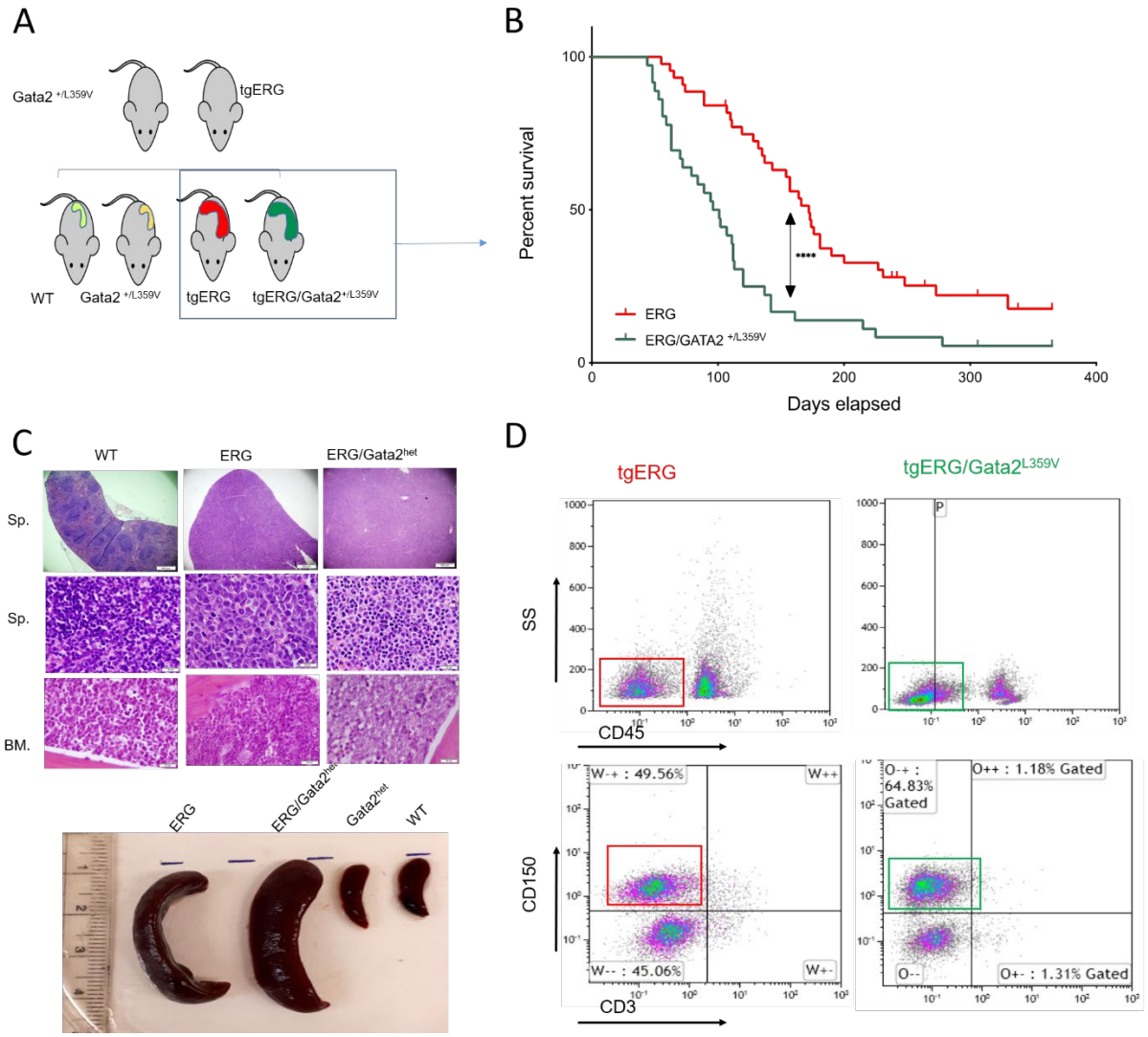

Figure. S1. **Accelerated leukemia and reduced survival in ERG/Gata2$^{+/L359V}$ mice. A.** Gata2$^{+/L359V}$ and tgERG mice mating strategy generates 4 different genotypes. **B.** tgERG/Gata2$^{+/L359V}$ double mutated mice, had shortened survival compared with tgERG littermates ($p<0.0001$, log rank Mantel-Cox test). **C.** Histopathological sections of tgERG/Gata2^{het} and tgERG leukemic mice. (up)-H & E stained histopathological sections of spleen and bone marrow demonstrated infiltrations of leukemic cells, (light microscope: upper panel 4X, middle and bottom panels 100X magnifications, scale bars calibrated as shown). (bottom) - Gross appearance of leukemia infiltrated spleens, alongside to normal sized spleens. Sp.- spleen BM- Bone marrow. **D.** Immunophenotype profile of the leukemia consisted of lineage negative, CD45^{dim} cells, expressing high level of CD150

A

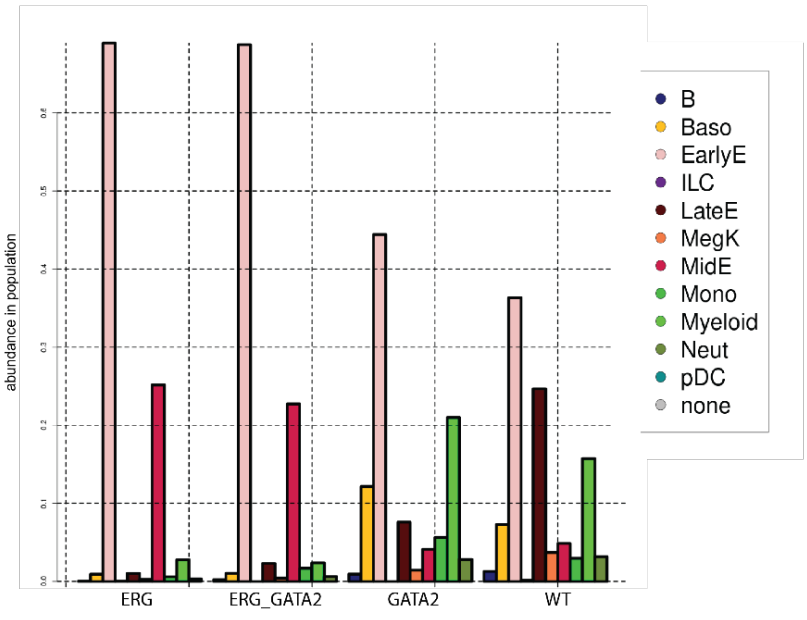

B

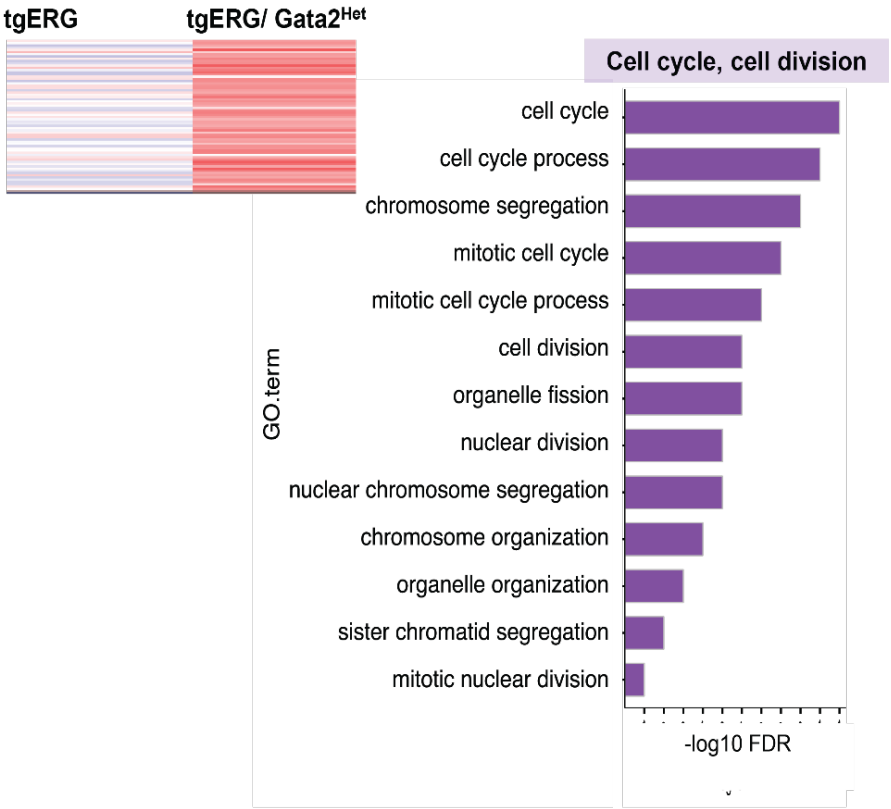

C

Aspm
Lbr
Cenpf
Nsl1
Mastl
Ckap5
Kif18a
Casc5
Wdr76
Cep152
Ncaph
Tpx2
Pola1
Kif4
Trim59
Golim4
Gabpb2
Hist2h2ac
Cenpe
Depdc1a
Melk
Smc2
Cdk5rap2
Mast2
Mtf1
Clspn
Dbf4
Ncapg
Pi4k2b
Cenpc1
Helq
Cit
Kntc1
Srrt
Rad18
Fancd2
Ccdc77
Ncapd2
Rad51ap1
Zfp626
Fanci
Prc1
Blm
Relt
Nup98
Rrm1
Ccp110
Ikzf5
Mki67
Mtfr2
Parpbp

Esco2
Anln
Ncapd3
Chek1
Kif23
Leo1
Ttk
Cep70
Cnot10
Kif15
Hmmr
Zfp672
Zfp39
Mis12
Spag5
Atad5
Cltc
Prr11
Top2a
Brca1
Idi1
Hist1h1b
Hist1h3i
Hist1h2ap
Hist1h2bj
Hist1h2ae
Hist1h4d
Hist1h1e
Hist1h3c
Hist1h3a
Hist1h1a
Hist1h2al
Zfp367
Cenph
Gen1
G2e3
Fancm
Mis18bp1
Ccdc88c
Smek1
Ncapg2
Rictor
6030458C11R
ik
Rad21
Senp1
Cbx5
Senp2
Pcyt1a
C330027C09R
ik
Pdpk1
Kat2b
Sgol1
Taf7
Cep76
Smc5
Fam122a
Kif11

Figure. S2. **10X RNAseq analysis reveals skewed differentiation and enhanced proliferation signature in tgERG/Gata2^{het} HSPCs**. **A.** Bar graph depicting abundance of population differentiation as reflected by gene expression pattern in the tested genotypes. **B.** illustration of k-means clustering of 10X RNAseq data, showing tgERG/Gata2^{het} HSPC highly express gene associated with 'Cell Cycle', and 'Cell Division' GO terms (K-means, an unsupervised algorithm that is used for cluster identification in a data set, was calculated with STRING platform[1]). **C.** List of genes clustered by k-means.

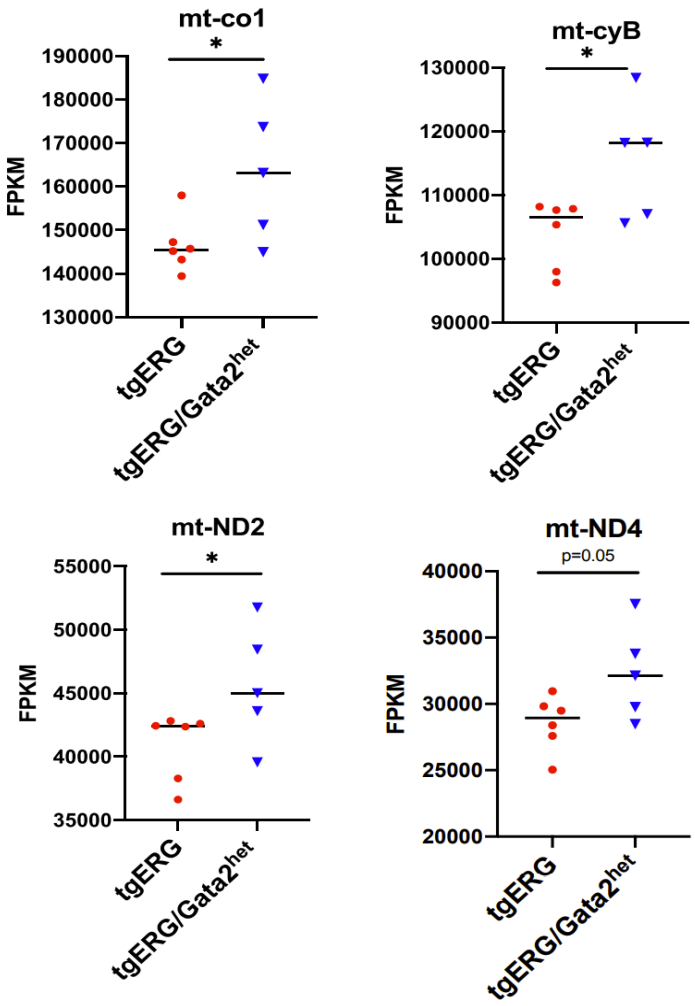

Figure S3. Selected mitochondrial genes upregulated in RNAseq of tgERG/Gata2^{het} pre-leukemia HSPCs. Individual mitochondrial genes (mt-co1: (Mitochondrially Encoded Cytochrome C Oxidase I),mt-cyB (Mitochondrially Encoded Cytochrome B), mt-ND2 (Mitochondrially Encoded NADH:Ubiquinone Oxidoreductase Core Subunit 2), mt-ND4 (Mitochondrially Encoded NADH:Ubiquinone Oxidoreductase Core Subunit 4) were differentially expressed in tgERG/Gata2^{het} samples (blue, n=5) compared with tgERG (red, n=6). (student t-test $p<0.05$, and in mtND4=0.05) FPKM- Fragments Per Kilobase of transcript per Million mapped reads.

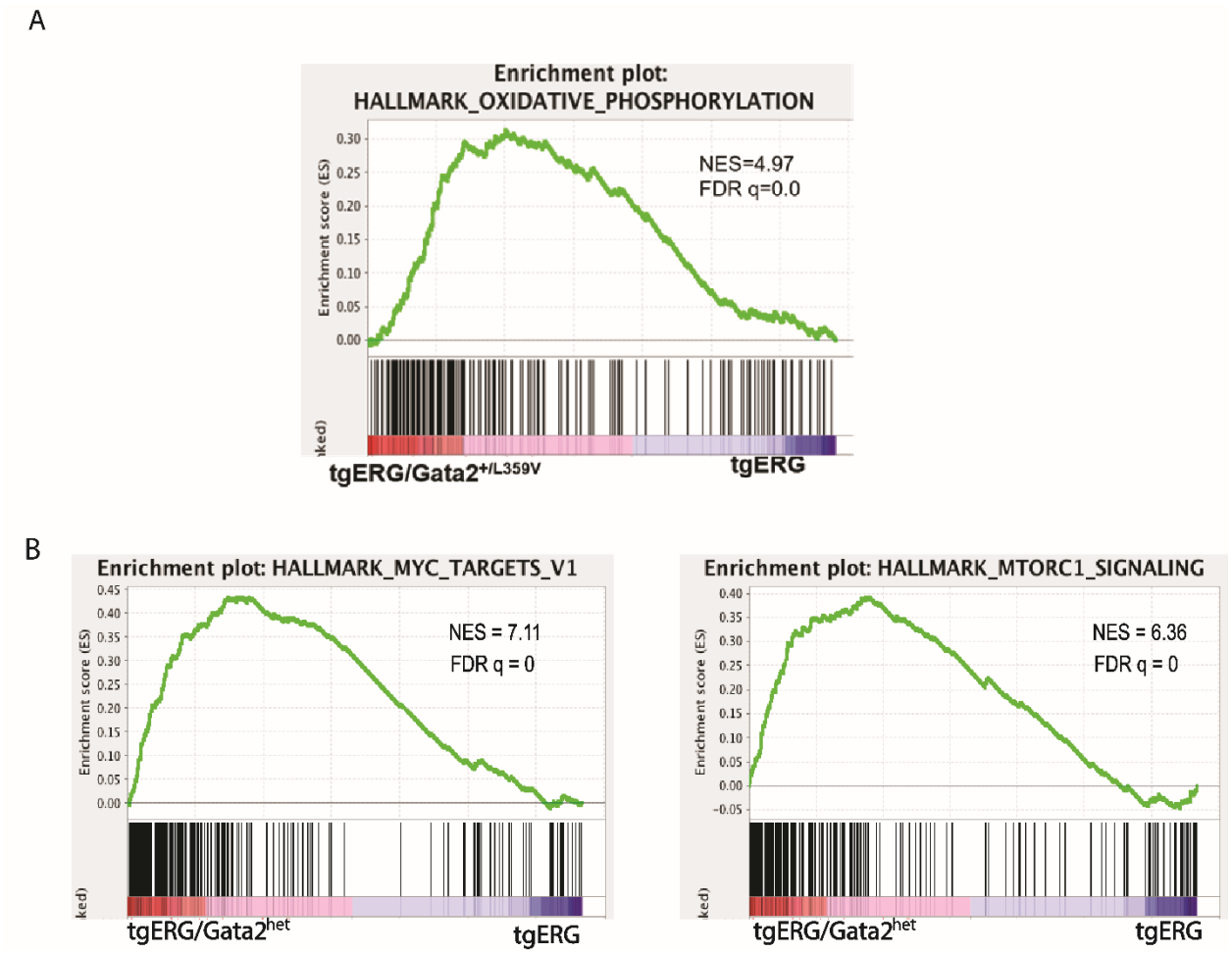

Figure S4. Expression signature enrichment in transgenic mice leukemic cells: A Gene set enrichment analysis of tgERG/Gata2+/L359V leukemic cells reviles that ‘Oxidative Phosphorylation’ pathway genes are enriched by gERG/Ga a2$^{+/L359V}$ expression. B Gene set enrichment analysis of ERG/Gata2^{het} leukemic cells revieles enrichment of MYC and mTOR signaling pathways genes (NES= normalized enrichment score, FDR= false discovery rate).

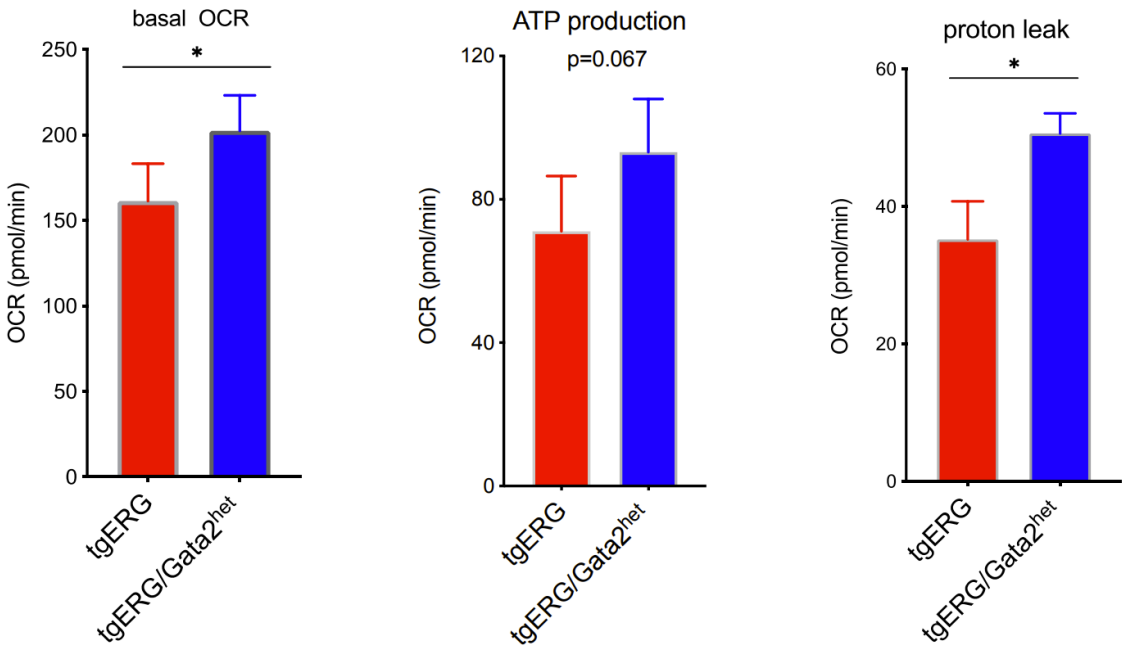

Figure S5. Increased Oxygen Consumption Rates of tgERG/Gata2^{het} HSPCs.

Basal oxygen consumption rates are significantly higher in tgERG/Gata2^{het} pre-leukemic HSPCs (**left**), and a trend (**middle**) of higher ATP production is also noted. Proton leak is shown to be higher in tgERG/Gata2^{het}, suggestive of an uncoupling effect of the respiratory chain (**right**). ($p<0.05$ n=3, two-tailed paired student t-test).

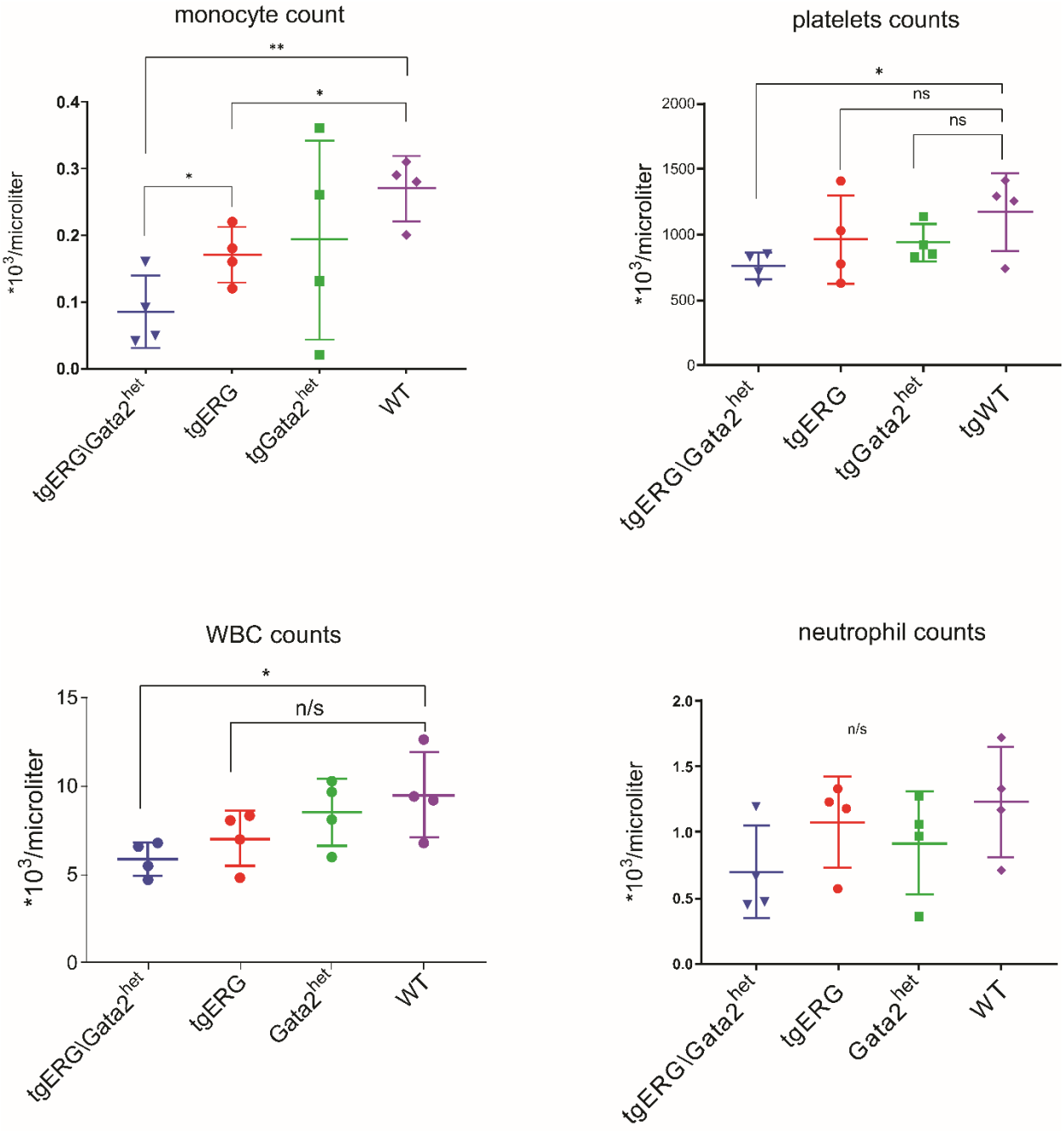

Figure. S6. tgERG/Gata2^{het} preleukemic mice develop blood cytopenia before clinical signs appear. Peripheral blood counts of 16 (4 of each genotype) preleukemic age- matched 6weeks old mice, showing that tgERG/Gata2^{het} encounter a decrease in several blood lineages before clinical signs are apparent. ($p<0.05$; one-way ANOVA).

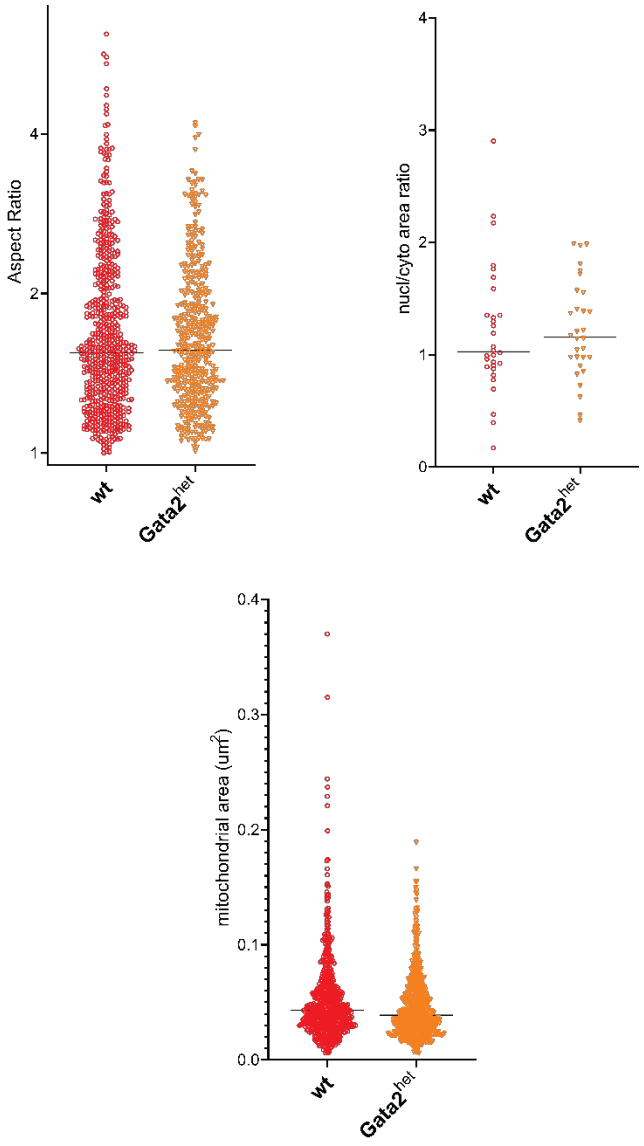

Figure S7. Lin- GATA2^{het} have normal mitochondrial morphology.

Transmission electrons microscopy captures imaging Analyses (NIH ImajeJ Fiji tool (50)) of lin- cells from BM of Gata2^{het} and wt 5 weeks old littermates ($n_{(mice)}$=3 $n_{(cells/mouse\ sample)}$=10 for both Gata2het and wt) Dot plots depicting aspect ratio (left) nucleos to cytoplasm area ratio (right) and mitochondrial area (bottom). No significant difference could be found in the measured mitochondrial parameters. (unpaired student T- test).

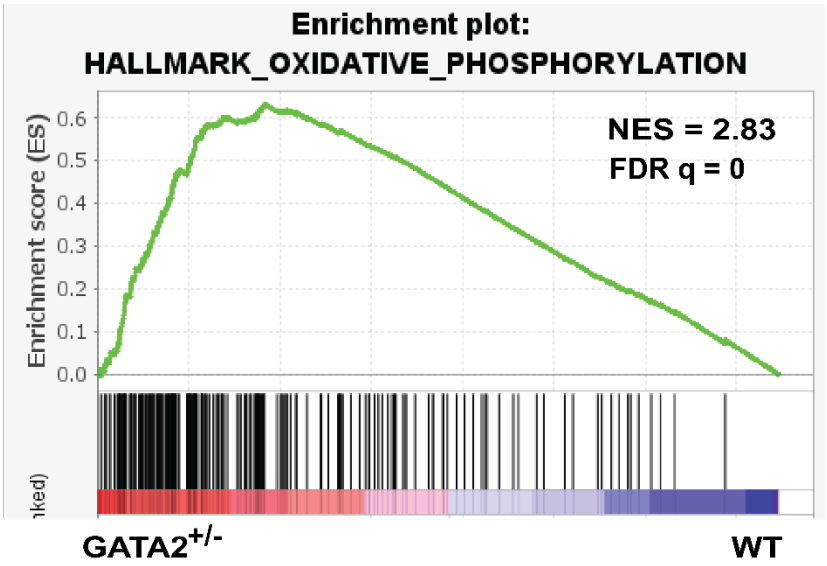

Figure S8. Oxidative Phosphorylation expression signature enrichment in GATA2het cells: Erythroid progenitor cells from GATA2het and wt background were subjected to RNA sequencing. Gene set enrichment analysis reveals enrichment in oxidative phosphorylation pathway genes.

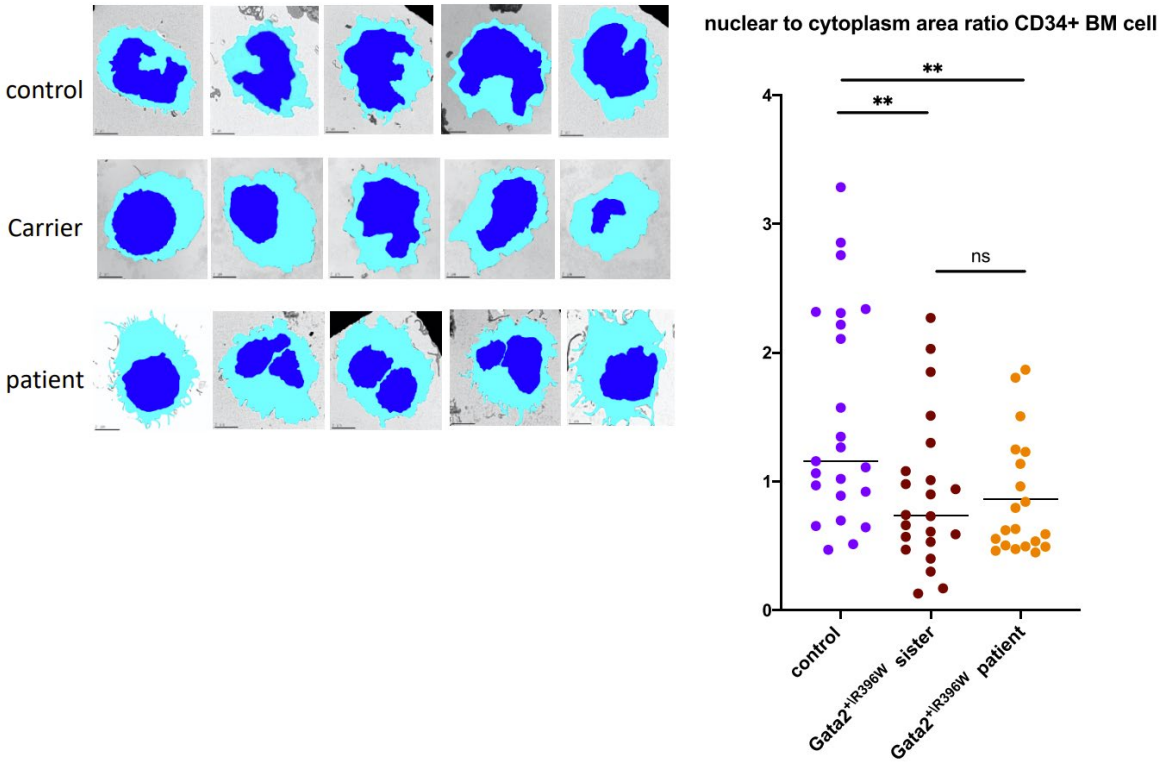

Figure S9. GATA2$^{+/R396W}$ CD34+ HSPCs display decreased nuclear to cytoplasm ratio. TEM imaging of GATA2$^{+/R396W}$ CD34+ HSPCs were analyzed using ImajeJ Fiji tool. Left - representative view of Nuclear to Cytoplasmic Ratio. Demarcation of cytoplasm (light blue) and nuclei (dark blue). CD34+ HSPCs from the GATA2$^{+/R396W}$ patient (lower panel), carrier sister (middle) and healthy donor (upper panel) were analyzed. (1:4 800-6 800 magnification scale, calibrated by Fiji tool). Right- Dot plots depicting nuclear to cytoplasm area ratio of CD34+ BM cells. Lines represent mean. A decreased nuclear to cytoplasmic ratio (NCR) was found in both the patient (orange) and the carrier sister (brown) compared to healthy donor (purple) (multiple student t-tests, n= $p<0.0001$).

Table S1- Flow cytometry antibodies

Target protein	Company	Catalog number	Conjugate	reactivity
cKit (CD117)	eBioscience	25-1172-82	PE-Cy5	Mouse
Sca1	eBioscience	56-5981-82	Alexa fluor 700	Mouse
Gr-1	Biolegend	108412	APC	Mouse
CD11b	BD	553311	PE	Mouse
CD41	Biolegend	133905	PE	Mouse
CD61	Biolegend	104315	APC	Mouse
CD150	Biolegend	115909	APC	Mouse
CD4	eBioscience	17-0041-82	APC	Mouse
SCA1	eBioscience	56-5981-82	Alexa fluor 700	Mouse
GR-1	Biolegend	108412	APC	Mouse
CD3	BD	555275	PE	Mouse
CD45	Biolegend	103114	PE-CY7	Mouse
CD8	Biolegend	100714	APC-CY7	Mouse
CD34	eBioscience	48-0341-82	efluor450	Mouse
7AAD	BD	51-68981		Mouse/Human
CD48	Biolegend	103418	Pacific blue	mouse

Table S2

Forward and reverse primers used for mtDNA/nDNA ratio:

16S rRNA forward and reverse primers

FWD: 5 -CCGCAAGGGAAAGATGAAAGAC-3

REV: 5 -TCGTTTGGTTTCGGGGTTTC-3

ND1 forward and reverse primers

FWD: 5 -CTAGCAGAAACAAACCGGGC-3

REV: 5 -CCGGCTGCGTATTCTACGTT-3

HK2 forward and reverse primers

FWD: 5 -GCCAGCCTCTCCTGATTTTAGTGT-3

REV: 5 -GGGAACACAAAAGACCTCTTCTGG-3

Supplemental Methods

Mouse models

ERG Tg mice model:

The *ERG* transgenic mice were generated by subcloning a 1.4-kb fragment of human ERG3 hematopoietic isoform into the HS21/45-*vav* vector [1]. This construct was microinjected into pronuclei of fertilized C57BL6 F1 oocytes and several founders were identified by PCR. All animals expressing ERG developed acute leukemia and died by the age of 7 months. Approximately 70% of leukemia were characterized as AML and approximately 30% as T-ALL [2]. DNA from tail clip of born mice is analyzed at the age of 4 weeks for the presence of human ERG by PCR.

$Gata2^{L359V}$ mice model:

Gata2-L359V knock-in murine model was generated by introducing the L359V mutation into the ZF2 domain, which is located in the exon 5 of the murine Gata2 gene. The Gata2-L359V knock-in mice were generated in C57BL/6 mice and on BALB/c background through backcross breeding. Gata2-L359V homozygous mutation resulted in embryonic lethality around E11.5 due to defects in primitive erythropoiesis and severe anemia. Gata2-L359V heterozygous adult mice exhibited defective hematopoietic development and block in the differentiation of chronic myeloid leukemia (CML) cells [3]. DNA from tail clip of born mice is analyzed at the age of 4 weeks for the presence of Gata2-L359V mutation by PCR.

$GATA2^{het}$ mice model:

Neomycin-resistant cassette replaced the carboxyl zinc finger domain of the murine GATA2 gene in a targeting vector with GATA2 complementary DNA sequence, generating a null mutation. Homozygous mice for GATA2 null died around E11.5. Mice

heterozygous for GATA2 appeared normal [4]. DNA from tail clip of born mice is analyzed by PCR at the age of 4 weeks for the presence of Neo sequence that is present in the knock-in construct.

tgERG/Gata2^{L359V} mice model:

Double transgenic mice were generated by crossing heterozygous TgERG mice [2] with *Gata2$^{+/L359V}$ knock-in* mice [3]. Four genotypes were identified by PCR analysis of DNA from tail clip of born mice at the age of 4 weeks using specific primers for Gata2-L359V mutation and specific primers for human ERG sequence - WT, tgERG, Gata2 L359V and the double transgene tgERG/Gata2 L359V.

tgERG/GATA2^{het} mice model:

Double transgenic mice were generated by crossing heterozygous TgERG mice [2] with *Gata2*$_{het}$ mice [4] . Four genotypes were identified by PCR analysis of DNA from tail clip of born mice at the age of 4 weeks using specific primers for the Neo sequence that is present in the knock-in construct and specific primers for human ERG sequence - WT, tgERG, Gata2 L359V and the double transgene tgERG/Gata2 L359V).

10X RNA sequencing and analysis

scRNA expression was obtained by using 10X to prepare cDNA library (Single Cell 3' Reagent Kits v2) the library was then sequenced on Illumina NextSeq 500 (paired end sequencing) Cell Ranger 3.0 (http://10xgenomics.com) was used to process Chromium single cell RNA-seq output, using mouse genome mm10 (version 1.2.0) as reference. The Metacell pipeline was used to derive informative genes and compute cell-to-cell similarity, K-nn graph covers and derive distribution of RNA in cohesive groups of cells and to derive strongly separated clusters using bootstrap analysis and computation of graph covers on resampled data. Default parameters were used unless otherwise stated. Cells with less than 500 UMI were discarded for low quality, retaining 12312 cells for further analysis, with a median 10010 UMI per cell. Raw data is available on GEO through accession GSE143308.

Oxygen consumption analysis

Oxygen Consumption Rates (OCR) was measured using the Seahorse XF96 Analyzer (Agilent Technologies, Santa Clara, California, USA). Cells were suspended in XF Assay Medium supplemented with 10 mM glucose,1 mM pyruvate, 2mM glutamine and 100 µM BSA-Oleate conjugate and seeded in a Seahorse XF96 cell culture plate (30-µl volume) precoated with Cell-Tak (Fisher Scientific). Cells were left to adhere for a minimum of 30 min in a CO2- free incubator at 37 °C, after which 150 µl of XF Assay Medium was added into each well. The plate was left to equilibrate for 20 min in the CO2-free incubator before being transferred to the Seahorse XF96 analyzer. Initial calibration experiments were performed to determine cell density, oligomycin and FCCP concentrations.

Optimal cell density was set to 200000 cells/well. Measurement of OCR was done at baseline and following sequential injections of (i) oligomycin (2 µM), an ATP synthase inhibitor, (ii) carbonyl cyanide-4 phenylhydrazone (FCCP) (20 µM), a mitochondrial uncoupler, and (iii) antimycin A (1 µM) and rotenone (1 µM), complex III and complex I inhibitors, respectively. All reagents were purchased from Sigma-Aldrich, St. Louis, Missouri, USA, aliquoted in DMSO in X1000 and diluted in assay media in the day of running the assay. OCRs were normalized by cell number.

RNAseq

For preparation of libraries the polyA fraction (mRNA) was purified from total RNA following by fragmentation and generation of double stranded cDNA. Then, end repair, A base addition, adapter ligation and PCR amplification steps were performed. Libraries were evaluated by Qubit (Thermo fisher scientific) and TapeStation (Agilent). Sequencing libraries were constructed with barcodes to allow multiplexing of 28 samples in 4 lanes. Around 22-28 million single-end 60bp reads were sequenced per sample on Illumina HiSeq 2500 V4 instrument. Poly-A/T

stretches and Illumina adapters were trimmed from the reads using cut adapt. Resulting reads shorter than 30bp were discarded.

Reads were mapped to Mus Musculus reference genome GRCm38 using STAR v2.4.2a, supplied with gene annotations downloaded from Ensemble release 82. Expression levels for each gene were quantified using HTseqcount. Differential expression analysis was performed using DESeq2. Raw P values were adjusted for multiple hypothesis using the Benjamini-Hochberg method. Raw data is available in GEO through accession GSE143238.

Immunophenotyping

BM cells were washed and stained with fluorochrome conjugated antibodies. Cells were washed and analyzed by Gallios 3 laser/10 colors Flow Cytometer (Beckman coulter, Brea, California, USA).

Leukemia panels: Progenitors: Lin(-) C-Kit, CD45, CD34 CD150, CD48, and Sca1; myeloid: CD13, CD11b CD14, GR-1 ; MegaErythroid: CD41 and CD61 together with Ter-119 ; T-Lymphoid: CD3, CD4, CD8, CD44 and CD25. Viability was assessed with 7AAD and dead cells were excluded by Kaluza software.

Cell proliferation assay

Tracing of cells generations was done using dye dilution assay using CFSE (Fisher Scientific, Waltham, Massachusetts, USA, #C34554), and analyzed using flow cytometry at 0h, 24h, 48h, 72h, and 96h. Dilution rate was calculated by Mean Fluorescence Intensity, and translated into Proliferation Index (P.I) using ModFit LT software (Verity Software House, Topsham, Maine, USA).

Gene Set Enrichment Analysis (GSEA)

PreRanked gene list analysis was performed. All the genes received per sample were scored by log10 P-values. Plus-sign was assigned for upregulated genes and

minus for downregulated genes. MSigDB: Molecular Signature DataBase of GSEA was used. The run was on classic mode. 500 permutations were defined.

Statistical analysis

All data are presented as mean and standard error of the mean (SEM). Statistical analyses were performed using GraphPad Prism® 8(La Jolla, CA, USA). Statistical significance of the data was assessed by two tailed Students *t*-test, or Mann-Whitney for two groups, and one way ANOVA, or Kruskal Wallis for more than two groups. Kaplan Meyer survival curves were generated by Log-Rank Mantel-Cox test. A *P*-value of <0.05 was considered significant.

Transmission electron microscopy

Cells were fixed in 2.5% Glutaralaldehyde in PBS over night at 4^0C, washed and post fixed in 1% OsO4 in PBS for 2h at 4^0C. Dehydration was carried out in graded ethanol followed by embedding in Glycid ether. Thin sections were mounted on Formvar/Carbon coated grids, stained with uranyl acetate and lead citrate and examined in Jeol 1400 Plus, transmission electron microscope (Jeol, Tokyo, Japan). Images were captured using SIS Megaview III and iTEM the Tem imaging platform (Olympus, Tokyo, Japan). All mice and human measurements and calculations in EM captures, were performed using Fiji open source platform for biological Image analysis. Analysis of patients bone marrow was approved by the IRB committee of Rabin Medical Center (approval 0840-18-RMC).

References

1. Ogilvy S, Metcalf D, Gibson L, Bath ML, Harris AW, Adams JM. Promoter elements of vav drive transgene expression in vivo throughout the hematopoietic compartment. *Blood*. 1999;94:1855-1863.
2. Thoms JA, Birger Y, Foster S, et al. ERG promotes T-acute lymphoblastic leukemia and is transcriptionally regulated in leukemic cells by a stem cell enhancer. *Blood*. 2011;117:7079-7089.
3. Fu YK, Tan Y, Wu B, et al. Gata2-L359V impairs primitive and definitive hematopoiesis and blocks cell differentiation in murine chronic myelogenous leukemia model. *Cell death & disease*. 2021;12:568.
4. Tsai FY, Keller G, Kuo FC, et al. An early haematopoietic defect in mice lacking the transcription factor GATA-2. *Nature*. 1994;371:221-226.